UPPSALA
UNIVERSITET

Digital Comprehensive Summaries of Uppsala Dissertations from the Faculty of Pharmacy 128

Development of Methods for Assessing Unbound Drug Exposure in the Brain

In vivo, in vitro and in silico

MARKUS FRIDÉN

ACTA
UNIVERSITATIS
UPSALIENSIS
UPPSALA
2010

ISSN 1651-6192
ISBN 978-91-554-7886-5
urn:nbn:se:uu:diva-130230

Dissertation presented at Uppsala University to be publicly examined in B22, Biomedicinskt Centrum, Husargatan 3, Uppsala, Friday, October 22, 2010 at 13:15 for the degree of Doctor of Philosophy (Faculty of Pharmacy). The examination will be conducted in English.

Abstract
Fridén, M. 2010. Development of Methods for Assessing Unbound Drug Exposure in the Brain. In vivo, in vitro and in silico. Acta Universitatis Upsaliensis. *Digital Comprehensive Summaries of Uppsala Dissertations from the Faculty of Pharmacy* 128. 72 pp. Uppsala. ISBN 978-91-554-7886-5.

The blood-brain barrier is formed by tightly joined capillary cells with transporter proteins and acts as to regulate the brain concentration of nutrients as well as many drugs. When developing central nervous system drugs it is necessary to measure the unbound drug concentration in the brain, i.e. the unbound brain exposure. This is to ensure that the drug reaches the site of action. Furthermore, when designing new drugs it is extremely valuable to be able to predict brain exposure from a tentative drug structure.

Established methods to measure total drug concentrations are of limited (if any) utility since the pharmacologically active, unbound, concentration is not obtained. The aim of the conducted research was to develop an efficient methodology to measure unbound drug in the brain and to generate a dataset for developing computational prediction models describing the relationship between drug structure and unbound brain exposure.

First it was demonstrated that unbound brain exposure can be efficiently assessed using a combination of total drug concentrations in the brain and separate measurements of drug binding in the brain slices. The in vitro brain slice method was refined and made high-throughput. Improvements were also made to the in vivo measurements of total concentrations by introducing an appropriate correction for drug in residual blood.

Modeling of a 43-drug dataset in the rat showed that unbound brain exposure is related to the drug hydrogen bonding potential and not to lipid solubility, which contrasts the common understanding. Further, the drug concentrations in cerebrospinal fluid approximated unbound concentrations in the brain (r^2=0.80) and were also correlated with corresponding measurements in humans (r^2=0.56). Therefore, rat-derived prediction models can be used when designing drugs for humans.

This thesis work has provided drug industry and academia with efficient tools to obtain and to use relevant estimates of drug exposure in the brain for evaluating drugs candidates.

Keywords: Blood-brain barrier, Drug transport, Tissue distribution, Transporters, Pharmacokinetics

Markus Fridén, Department of Pharmaceutical Biosciences, Box 591, Uppsala University, SE-75124 Uppsala, Sweden

ISSN 1651-6192
ISBN 978-91-554-7886-5
urn:nbn:se:uu:diva-130230 (http://urn.kb.se/resolve?urn=urn:nbn:se:uu:diva-130230)

You must unlearn what you have learned.

Yoda, Star Wars Trilogy, Episode V

List of Papers

This thesis is based on the following papers, which are referred to in the text by their Roman numerals.

I **In vitro methods for estimating unbound drug concentrations in the brain interstitial and intracellular fluids.**
Fridén M, Gupta A, Antonsson M, Bredberg U, Hammarlund-Udenaes M. *Drug Metab Dispos*, 2007, 35:1711-9. © 2007 The American Society for Pharmacology and Experimental Therapeutics.

II **Development of a high-throughput brain slice method for studying drug distribution in the central nervous system.**
Fridén M, Ducrozet F, Middleton B, Antonsson M, Bredberg U, Hammarlund-Udenaes M. *Drug Metab Dispos*, 2009, 37:1226-33. © 2009 The American Society for Pharmacology and Experimental Therapeutics.

III **Improved measurement of drug exposure in brain using drug-specific correction for residual blood.**
Fridén M, Ljungqvist H, Middleton B, Bredberg U, Hammarlund-Udenaes M. *J Cereb Blood Flow Metab,* 2010, 30:150-61. © 2009 International Society for Cerebral Blood Flow and Metabolism.

IV **Structure-brain exposure relationships in rat and human using a novel data set of unbound drug concentrations in brain interstitial and cerebrospinal fluids.**
Fridén M, Winiwarter S, Jerndal G, Bengtsson O, Wan H, Bredberg U, Hammarlund-Udenaes M, Antonsson M. *J Med Chem*, 2009, 52:6233-43. © 2009 American Chemical Society.

Reprints were made with permission from the respective publishers.

Related publications

On the Rate and Extent of Drug Delivery to the Brain.
Hammarlund-Udenaes M, Fridén M, Syvänen S, Gupta A. *Pharm Res.* 2008, 25:1737-50.

Methodologies to assess brain drug delivery in lead optimization.
Hammarlund-Udenaes M, Bredberg U, Fridén M. *Curr Top Med Chem.* 2009, 9:148-62.

Measurement of Unbound Drug Exposure in Brain: Modelling of pH Partitioning Explains Diverging Results between the Brain Slice and Brain Homogenate Methods.
Fridén M, Bergström F, Wan H, Rehngren M, Ahlin G, Hammarlund-Udenaes M, Bredberg U. *Submitted.*

Contents

1 Introduction 11
1.1 Physiology of the brain and its barriers 12
1.2 Drug disposition in the brain 13
1.2.1 Diffusion and passive permeability 14
1.2.2 Carrier-mediated transport 15
1.2.3 Elimination by ISF bulk flow 17
1.2.4 Drug metabolism in the brain 17
1.2.5 Distribution within the brain 17
1.2.6 Diffusion in the brain interstitial space 18
1.2.7 Plasma protein binding 19
1.2.8 Integrated analysis of drug disposition in the brain 19
1.3 Methodologies for measurement of BBB transport 22
1.3.1 Rate of BBB transport 22
1.3.2 Extent of BBB transport 23
1.3.3 *In vitro* methods 26
1.4 Methodologies for prediction of brain exposure 27
1.4.1 Computational model development 27
1.4.2 Overview of BBB prediction models 29
1.5 Translation to humans 30

2 Aims of the thesis 32

3 Methods 33
3.1 Animals 33
3.2 Animal surgery 33
3.3 Compound selection 33
3.4 Determination of intra-brain distribution, $V_{u,brain}$ 35
3.4.1 *In vivo* microdialysis 35
3.4.2 *In vitro* brain slice method 36
3.4.3 *In vitro* brain homogenate binding method 36
3.5 Measurement of $K_{p,uu,brain}$ and $K_{p,uu,CSF}$ *in vivo* 37
3.6 Computational modeling 38
3.6.1 Molecular descriptors 38
3.6.2 PLS modeling 39
3.7 Bioanalytical methods 39
3.7.1 Technical procedures 39

3.7.2 Drug quantification 40
3.8 Statistical analysis 41
3.8.1 Method comparison using Altman and Bland analysis 41
3.8.2 Statistical modeling of variance components 41
3.8.3 The propagation of error method 41
3.8.4 Statistical tools for computational modeling 42

4 Results and discussion 43
4.1 Evaluation of *in vitro* measurements of $V_{u,brain}$ 43
4.2 Unbound intracellular drug concentrations 45
4.3 Optimization of the brain slice method 45
4.4 Development of a correction model for drug in residual blood 47
4.5 Structure - brain exposure relationships 49
4.5.1 *In silico* models for $K_{p,uu,brain}$ 50
4.5.2 *In silico* models for $K_{p,brain}$ (logBB) 52
4.6 Utility of $K_{p,uu,CSF}$ as a surrogate for $K_{p,uu,brain}$ in the rat 53
4.7 Agreement between $K_{p,uu,CSF}$ in rat and humans 56

5 Conclusions and perspectives 58

6 Populärvetenskaplig sammanfattning 60

7 Acknowledgements 63

8 References 66

Abbreviations

A_{brain}	Amount of drug in brain tissue excluding vascular spaces
ACDLogD7.4	Calculated octanol-water partitioning coefficient at pH 7.4
ACDLogP	Calculated octanol-water partitioning coefficient
$AUC_{u,brainISF}$	Area under curve of $C_{u,brainISF}$ vs. time plot
$AUC_{u,p}$	Area under curve of $C_{u,p}$ vs. time plot
BBB	Blood-brain barrier
BCRP	Breast Cancer Resistance Protein
BCSFB	Blood-CSF Barrier
C_{blood}	Total drug concentration in blood
$C_{brain,h}$	Drug concentration in diluted brain homogenate sample
C_{CSF}	Total drug concentration in CSF
C_p	Total drug concentration in plasma
$CL_{bulkflow}$	Drug clearance by bulk flow of brain interstitial fluid
CL_{efflux}	Net BBB efflux clearance by active transport
CL_{in}	Net BBB influx clearance
CL_{influx}	Net BBB influx clearance by active transport
CL_{met}	Elimination clearance from brain due to metabolism
$CL_{passive}$	Passive BBB transport clearance
CL_{out}	Net BBB efflux clearance
ClogP	Calculated octanol-water partitioning coefficient
C_p	Total drug concentration in plasma
CNS	Central nervous system
CSF	Cerebrospinal fluid
$C_{u,brainISF}$	Unbound drug concentration in brain interstitial fluid
$C_{u,cell}$	Unbound drug concentration in intracellular fluid
$C_{u,CSF}$	Unbound drug concentration in cerebrospinal fluid
$C_{u,p}$	Unbound drug concentration in plasma
$f_{u,brain}$	Unbound fraction of drug in brain homogenate
$f_{u,hD}$	Unbound fraction of drug in diluted brain homogenate
$f_{u,CSF}$	Unbound fraction of drug in cerebrospinal fluid
$f_{u,p}$	Unbound fraction of drug in plasma
HBA	Number of hydrogen bond acceptors
HBD	Number of hydrogen bond donors
Hct	Arterial hematocrit
$K_{p,brain}$	Total brain-to-plasma concentration ratio
$K_{p,uu,brain}$	Unbound brain-to-plasma concentration ratio

$K_{p,uu,cell}$	Unbound intra-to-extracellular concentration ratio
$K_{p,uu,CSF}$	Unbound cerebrospinal fluid-to-plasma concentration ratio
logBB	Logarithm of $K_{p,brain}$
LogUnionized	Logarithm of the fraction of molecules that are unionized
MRP	Multidrug Resistance-associated Protein
MW	Molecular weight (Da)
NPSA	Van der Waals non-polar surface area
OAT	Organic Anion Transporter
PCA	Principal Component Analysis
Pgp	P-glycoprotein
PLS	Projections to Latent Structures
PSA	Van der Waals polar surface area
Q_{alb}	Cerebrospinal fluid-to-plasma concentration ratio of albumin
RingCount	Number of rings in a molecule
RMSE	Root of mean squared error
RotBond	Number of rotatable bonds
V_{eff}	Effective vascular plasma space of a drug (μL/g_brain)
V_{er}	Volume of erythrocytes in brain vascular space (μL/g_brain)
VOL	Molecular volume
$V_{protein}$	Apparent vascular space of plasma proteins (μL/g_brain)
$V_{u,brain}$	Unbound volume of distribution in brain (μL/g_brain)
V_{water}	Apparent vascular space of plasma water (μL/g_brain)

1 Introduction

Whether a drug is taken orally or parenterally by injection, the blood circulation carries the drug molecules to the capillaries of every organ and tissue of the body. The drug then easily diffuses out of capillaries into most tissues. From the random nature of diffusion it can be inferred that over time, the concentration of freely diffusible, *unbound*, drug is similar throughout the body. The brain is an important exception, because the random passive movement of drug is restricted by the so called blood-brain barrier (BBB) in favor of active and directional drug transport mediated by specific transport proteins. This commonly, but not always, results in the maintenance of unbound drug concentrations in the brain that are lower than the corresponding concentration in blood plasma or other organs.

For a drug to evoke its pharmacologic effect in the brain it is obvious that, following a tolerably small dose, the concentration of unbound drug needs to be high enough to efficiently bind to and thus act on the target protein. Equally, there can be benefit from the BBB for drugs acting in other organs, since side effects in the brain can be avoided. It is essential to obtain an understanding of the processes governing drug exposure in the brain and to address these in the chemical design of the drug in order to develop effective drug treatments. Yet there is little known about the relationship between the chemical structure of the drug and the level of drug exposure in the brain. A major impediment for this understanding has been the lack of experimental methods to actually measure the unbound drug. Principally all analytical methods are limited to measuring the total drug concentration i.e. the total amount of drug in a tissue sample. This can be very misleading since the unbound drug only represents an unknown fraction, the remainder being inactive drug deposited in the cells.

By dialysis of diffusible drug using the microdialysis technique it is possible to measure unbound drug *in vivo*. Unfortunately, microdialysis has technical challenges that preclude implementation in drug discovery. This is because discovery programs need to quickly study large numbers of drug compounds in order to build structure-brain exposure relationships and to select the most appropriate molecules for further development. Following the development of the more efficient methodologies presented in this thesis, comes the possibility of incorporating un-ambiguous data on brain exposure in the design of safe and efficacious drugs.

1.1 Physiology of the brain and its barriers

Owing to the high rate of energy metabolism of the brain, it is one of the most highly perfused organs. While representing only 2 % of the total body volume it receives as much as 12 % of the cardiac output [1]. The limited distances that oxygen and nutrients can cover by diffusion through tissue is balanced by the incredible density of the capillary network. The average distance between a neuron and a microvessel in gray matter is ~20 μm [2, 3], and it has been said that virtually every neuron is supplied with its own capillary [4]. Depending on intake of food and liquid as well as external stress factors, there are large variations in the composition of blood in terms of the concentrations of ions, nutrients and neurotransmitters. These fluctuations are incompatible with the functions of the brain, which are highly reliant on regulated flows of ions across and along neurons. In order to create a constant environment within the brain, the specialized brain capillary network is forming the BBB by tight association of cells using protein complexes known as tight-junctions. Each endothelial cell has a luminal phospholipid cell membrane, facing the blood, and an abluminal membrane, facing the brain. Water soluble nutrients such as glucose and amino acids cannot cross these lipid membranes at a rate that is fast enough to keep up with rate of metabolism. Therefore, the BBB is complemented with numerous transmembrane transport proteins that facilitate and control the entry of nutrients as well as disposal of metabolites.

Many of these transporters have the capability to transport also molecules that are foreign to the body, such as drugs, if there is resemblance in the chemical structure. While this conceivably contributes to the delivery of drugs to the brain, the more commonly observed situation is that BBB limits the access to the brain by efficient efflux transporters that pump the drug back into blood. The role of drug transporters for drug exposure in the brain is discussed in more detail in Section 1.2.2.

The brain is very heterogeneous and has an anatomy of its own describing different regions and structures with various functions. The cerebrospinal fluid (CSF) in which the brain is suspended is of particular interest for measurement of drug exposure since it can be readily sampled. CSF is produced by a leaf-like and highly vascularized organ, the choroid plexus (CP), located in the ventricular cavities of the brain. The CP is the interface between blood and the CSF and has a barrier function similar to the BBB. It is therefore referred to as the blood-CSF barrier (BCSFB). Unlike the BBB there are large pores between the endothelial cells of the BCSFB; the barrier function arises from a layer of tightly joined epithelial cells facing the CSF (Fig. 1). The CSF is produced at a rate of 2-5 μL/min in the rat [5] and flows through the ventricles which are connected with the subarachnoid space on the surface of the brain. The majority of produced CSF is reabsorbed by outcroppings (villi) of the arachnoid membrane, whereas a small portion of CSF

descends down the spinal cord through the central canal. Due to the leaky gap-junctions between the ependymal cells of ventricular lining there is no actual barrier to diffusion of drug from CSF to brain tissue or in the opposite direction.

Similar to the CSF, but much smaller in magnitude, is the bulk flow of brain tissue interstitial fluid (ISF). The ISF is produced at the BBB as well as by metabolism of glucose [6] and takes special pathways in the space around capillaries and larger vessels. The ISF bulk flow drains in the CSF.

The brain is heterogeneous also on the microscopic scale having different cell types intertwined such as neurons, astrocytes and microglia. Collectively, the cells make up about 80 % of the brain tissue volume in which the remaining 20% is interstitial space containing ISF. Although the ISF behaves like a salt solution in terms of drug diffusion, it is physically a gel of hydrated polysaccharides and fibrous protein [7]. The chemical composition of brain is approximately 80 % water, 10 % proteins and 10 % lipids and solutes.

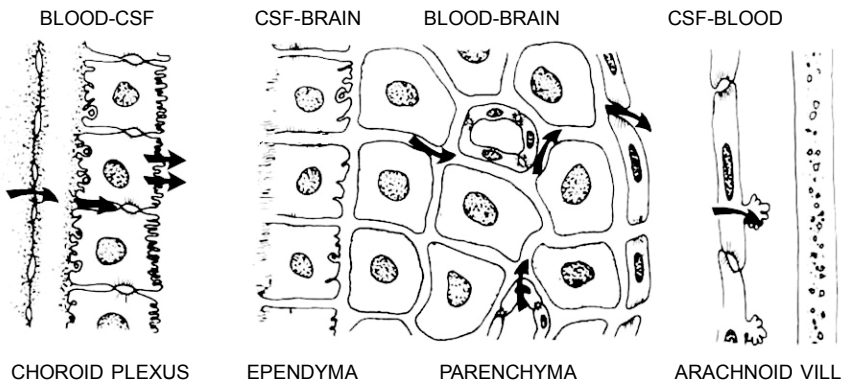

Figure 1. Diagram of interfaces in the brain. CSF is produced by the choroid plexus (left) and flows through the ventricles to the subarachnoid space surrounding the brain, where it is reabsorbed by arachnoid villi (right). Interstitial fluid originates from the brain capillaries shown as 2 circular structures (center) and joins the CSF flow in the ventricles and subarachnoid space. (From ref [8] with permission).

1.2 Drug disposition in the brain

This section gives an introduction to current understanding of drug disposition in the brain. It encompasses processes at the BBB that either add or remove drug from the brain as well as processes that describe the fate of the drug once inside the brain. For the presentation of each process, particular focus is put on the effects on the unbound drug concentration in the brain ISF (Fig 2). The section concludes with an integrated analysis of all

processes, which is a requirement for understanding the overall picture of drug disposition in the brain.

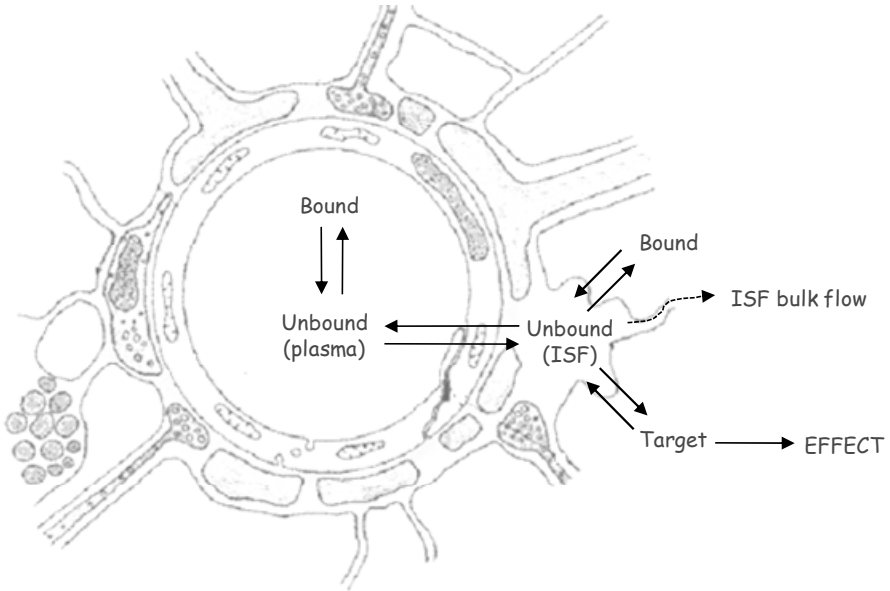

Figure 2. Drug circulates in the blood as free drug and drug bound to plasma proteins. The concentration of unbound drug in plasma drives the transport across the BBB into the brain interstitial space where the drug resides or binds to brain cells. The unbound drug molecules in the brain interstitial fluid are pharmacologically active since they are available to bind the target and elicit the effect. Elimination of drug from brain by transport across the BBB can only occur for unbound drug molecules in the brain interstitial space. Hence, the BBB acts only as to regulate the unbound drug concentration in the brain ISF relative to the unbound drug concentration in blood plasma. In contrast, the commonly measured total drug concentration in the brain is highly dependent on the extent of drug binding in brain tissue, which is a process distinct from BBB transport. (Adapted from ref [9] with permission).

1.2.1 Diffusion and passive permeability

Drug molecules have no clue where they are headed. By diffusion they move in random patterns through the water as determined by seemingly incidental movements of adjacent water molecules. There is no favored direction of diffusion for any one drug molecule. However, when several molecules are present at high concentration in one location there is always net movement of drug towards locations with lower concentrations. This intuitive and predictable phenomenon is a consequence of statistical probability. It is simply more likely that at least one molecule will move from a location of high concentration to a location of low concentration, than it is for a molecule to move in the opposite direction. Provided enough time, differences in concentration diminish. Passive diffusion of drug across the BBB is likewise *sym-*

metric by the same principle, though the rate of diffusion can be dramatically reduced. Even so, by providing enough time all drugs would be expected to reach the same concentrations in the brain as in blood had it not been for additional dispositional processes that introduce *asymmetry* in BBB transport (see Section 1.2.2).

There is a strong relationship between the lipid solubility of the drug (lipophilicity) and its rate of permeating the BBB (permeability), where increased lipophilicity is associated with increased permeability [10]. This relationship is related to the partitioning of drug into the lipid membrane, which is needed for permeation. Molecular size is an additional factor since physical work is needed to create the pocket in the lipid membrane with its surface tension [11]. Acid-base properties are also related to passive permeability. It is generally held that it is the uncharged forms of weakly basic and acidic drugs that dominate passive membrane permeation. Hence, the proton dissociation constant, pKa, in relation the physiological pH (7.4) will also influence passive permeability.

1.2.2 Carrier-mediated transport

Endogenous compounds and hydrophilic drugs that do not readily partition into the membranes of the BBB may still be transported into the brain by carrier proteins called transporters. For more permeable drugs, carrier-mediated transport commonly occurs simultaneously with passive transport. Based on the direction of transport across the BBB, transporters are termed as influx (blood to brain) or efflux (brain to blood) transporters. Some transporters can mediate transport in both directions. Principal modes of carrier-mediated transport of small molecules can be identified (Fig. 3).

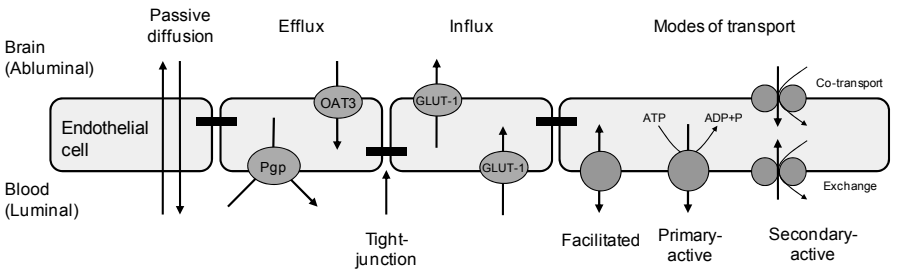

Figure 3. Drug transport mechanisms at the blood-brain barrier.

1.2.2.1 Facilitated transport

Facilitating transporters increase the rate of passive diffusion through the membrane by acting as a pore which is selective for the particular solute. There is no energy consumed by this mode of transport, thus net transport only occurs in the downhill direction of a concentration gradient. Some

members of the solute carrier (SLC) family of transporters function in this mode. For example the glucose transporter (GLUT1, SLClC2A1), which is the most abundant transporter in the BBB, has been proposed to facilitate the diffusion of morphine-6-glucuronide into the brain [12]. Similarly, the system L-amino acid transporter (LAT1, SLC7A5) transports gabapentin into the brain [13].

1.2.2.2 Active transport

Active transport is paramount for drug exposure in the brain since it is the only way to transport drug asymmetrically i.e. against a concentration gradient. Depending on the source of energy, active transport can be categorized as primary or secondary-active [14]. Primary active transport is mediated by members of the ATP-binding cassette transporter family i.e. ABC-transporters, which utilize the direct hydrolysis of ATP for the translocation of a drug.

According to current understanding P-glycoprotein (Pgp, ABCB1) is the single most important transporter for limiting the brain exposure of commonly used drugs. A most compelling example of Pgp effects on drug pharmacology is provided by the opioid drug loperamide. While loperamide has the typical constipating effect of an opioid, its limited brain exposure and thus limited central effects makes it an effective and safe anti-motility agent. Pgp is a transmembrane protein which is present at the luminal membrane of the BBB facing the blood side. It binds and translocates its substrates from the inner leaflet of the lipid bi-layer and releases the substrate to the outer leaflet or directly in the capillary lumen [15]. The substrate specificity of Pgp is tremendously broad and it has been proposed that the only requirement is a degree of hydrogen bonding [16]. The ABC super-family of transporters also include multidrug resistance-associated proteins (MRPs) of which the isoforms MRP1, MRP4 and MRP5 are expressed at the BBB. MRP transports acidic drugs, various drug conjugates as well as nucleosides. While the presence of the breast cancer resistance-associated protein BCRP (ABCG2) is long known, its importance for drug efflux has been a matter of debate. The situation was recently clarified by showing that the BCRP effect *in vivo* can be effectively masked by Pgp due overlapping substrate specificity [17, 18].

Secondary-active transporters utilize the hydrolysis of ATP indirectly by relying on an ATP-dependent concentration gradient of another solute such as sodium. The organic anion transporter OAT3 (SLC22A8) is a secondary-active transporter present in the abluminal membrane facing the brain side. OAT3 is involved in the efflux of benzyl-penicillin [19] as well as endogenous metabolites [20, 21].

1.2.3 Elimination by ISF bulk flow

In contrast to both passive diffusion and carrier-mediated transport, the elimination of drug by bulk flow of brain ISF makes no distinction with regards to the structure or properties of the drug. In fact, the concept of ISF bulk flow was used to explain the equal rates of elimination of differently sized polymers [22, 23]. ISF bulk flow has a conceptual key role in drug disposition in the brain, since it provides a basal rate of elimination for all drugs. The magnitude of ISF bulk flow is however very small; most of the reported values range between 0.1 and 0.3 μL/g_brain in anaesthetized rats [23, 24]. A slightly higher value (0.6 μL/g_brain) was obtained in one study with conscious rats [25].

1.2.4 Drug metabolism in the brain

The expression level of cytochrome P450 enzymes in brain tissue is at least 10-fold lower than in the liver. However, there are large variations between brain regions and also brain cells [26]. The drug metabolizing CYP isoform CYP2D6 has been of particular interest since it is expressed within individual brain cells at levels similar to the liver [27] and is involved in the metabolism of many centrally acting drugs including codeine and antidepressants.

Although the levels of enzymes are generally not as high as in the liver it can be argued that, in analogy to intestinal first-pass metabolism, the BBB would be a very strategic location to eliminate drug and may significantly limit drug exposure in the brain. However, extensive oxidative metabolism occurring at the BBB would put the whole brain at risk of reactive metabolites and reduced barrier function. Efficient drug efflux seems to be a safer mechanism to protect the brain. The difficulty in appreciating the (lack of) importance of metabolism to drug elimination from brain is related to the lack of *in vivo* methods that distinguish between metabolism and carrier-mediated efflux, or between metabolism in the brain and in the periphery with subsequent transport of the metabolites into the brain.

In general, pharmacological or toxicological consequences of drug metabolism in the brain are more likely to be related to the metabolites that are formed than the elimination of parent drug from the brain.

1.2.5 Distribution within the brain

The distribution of drug that occurs within the brain, after the drug has reached there, is often referred to as “tissue binding”. It involves the uptake of drug from the interstitial space into cells where it binds to various cell constituents. Drug is also bound on the outside of the cell membranes, however this membrane surface area represents no more than 0.5 % of the total membrane surface area of the cell [28]. A common misconception is that

drug is eliminated from brain ISF by uptake into cells. Cellular uptake and non-specific tissue binding is generally a reversible process, which means in this case that the drug molecule eventually returns to the ISF. Hence, there is no net effect when the unbound brain ISF concentration is averaged over time. The total brain tissue concentration on the other hand is highly dependent on binding in cells. A relationship can be defined between the unbound drug concentration in the brain ISF ($C_{u,brainISF}$) and the amount of drug (total drug concentration) in the brain (A_{brain}). This relation is unique for every drug and is described by *the unbound volume of distribution in brain* ($V_{u,brain}$, [29]):

$$V_{u,brain} = \frac{A_{brain}}{C_{u,brainISF}} \quad (1)$$

$V_{u,brain}$ is an apparent volume in which a known amount of drug (A_{brain}) appears to be dissolved. Its inverse value can also be understood as an unbound fraction of drug in the brain. The smallest possible value for $V_{u,brain}$ is the physical volume of brain interstitial fluid i.e. 0.2 mL/g_brain. This is only seen if the drug does not at all enter brain cells but is only present in the interstitial space. Higher values of $V_{u,brain}$ are obtained for drugs that enter cells to a greater extent. Particularly large values occur when the drug is extensively bound to cell constituents.

$V_{u,brain}$ is a main theme of this thesis for a particular reason; if the value of $V_{u,brain}$ is determined for a drug, it can be used to calculate $C_{u,brainISF}$ from measured values of A_{brain}. As discussed above, $C_{u,brainISF}$ is the pharmacologically "active" concentration, given that the site of action is facing the ISF, and therefore the relevant measure of brain exposure. The measured total concentration (A_{brain}) on the other hand, mainly reflects inactive, non-specifically bound drug.

1.2.6 Diffusion in the brain interstitial space

The interstitial space containing the ISF is continuous throughout the brain and allows all drug molecules to be transported by diffusion. The rate of diffusion depends on the size of the molecule. The diffusion is also hindered for molecules that do not easily enter cells since longer distances need to be covered. As result of the increased path length the effective diffusion coefficient in tissue for such molecules is reduced by a factor ~2.6 [7]. In terms of the rate of drug entry into brain, diffusion through interstitial space is implicitly considered a fast process since the distances to be covered are very small due to the proximity between microvessels. Interstitial space diffusion occurs only within the brain; hence it does not result in net clearance of drug. Brain regions adjacent to ventricles and the subarachnoid space may consti-

tute a special case, since diffusion of solutes to and from CSF occurs across the ependymal lining (see Section 1.1).

1.2.7 Plasma protein binding

Plasma protein binding has essentially no direct role for the disposition of drugs in the brain. It is mentioned in this context because in order to determine whether the drug exposure in the brain is "high" or "low" $C_{u,brainISF}$ needs to be compared with the corresponding unbound concentration in plasma (see Section 1.2.8). Since the total plasma concentration is the measured entity, plasma protein binding becomes an issue when estimating the unbound plasma concentration. With that said, it is to be noted that the unbound fraction in plasma has no effect on the steady state unbound plasma concentration of any oral drug or parenterally given low-extraction drug. As a philosophical note, had we been fortunate enough to start out our research on drug disposition with analytical tools capable of measuring the unbound drug, we might not ever have made the connection between plasma protein binding and BBB transport.

1.2.8 Integrated analysis of drug disposition in the brain

As described in the sections above numerous processes are involved in brain disposition of drugs, some of which can be directly studied or predicted from the chemical properties of the drug. The impact on brain exposure of an individual dispositional process may seem straightforward at a first consideration. For example, regarding the passive permeation from blood to brain; it may appear logic that a higher rate of passive transport into the brain translates into more drug in the brain. This is essentially incorrect because the gain is inevitably offset by the accompanying increased outward passive transport. As illustrated, concerted actions of several processes with interrelationships can cause surprising phenomena to occur.

Clearly, the human mind has limited ability to predict the behavior of complex systems. Rather than simplifying the problem by focusing on particular parts of the system, it is a better idea to approach the whole problem by making a *model*. A model of drug disposition in the brain can be constructed by mathematically describing the individual processes as they are understood and by appropriately inter-connecting them. The model can then be used, with our without the help of computers, to *simulate* the behavior of the whole system under various conditions. The use of modeling and simulation are standard pharmacokinetic tools for describing drug disposition in the body as a whole, and the extension to the brain is done using the same principles. The following describes an integrated analysis of drug disposition in the brain, much of which permeates views and ideas presented in this thesis.

Processes are described by models in a quantitative manner using *parameters* that can attain various numerical values. One such parameter is the passive transport clearance across the BBB ($CL_{passive}$), which describes how fast the drug is passively transported across the BBB. $CL_{passive}$ is given in units of flow and is interpreted as a volume of blood plasma per unit of time which is completely cleared from drug by means of transport across the BBB. For the model which is considered here (Fig. 4), the drug is being passively transported from the blood compartment to a single brain compartment by the efficiency given by $CL_{passive}$.

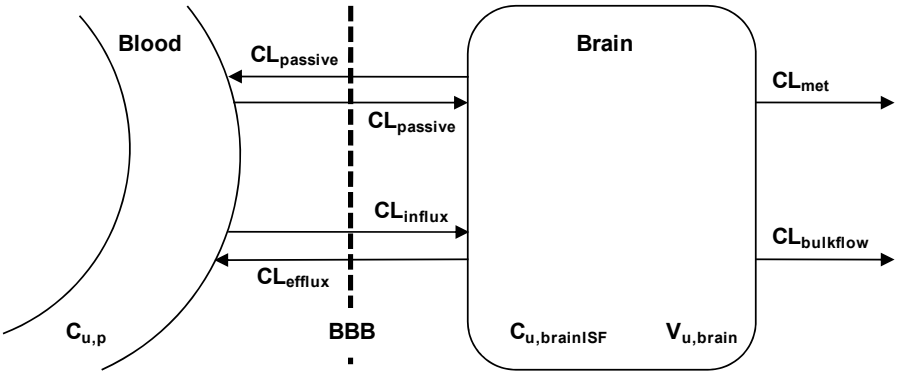

Figure 4. Schematic representation of drug disposition in the brain. See text for details.

Whether the drug moves across the BBB from blood to brain or in the opposite direction, the very same membranes need to be crossed. Therefore, passive transport in the direction of brain to blood is equally efficient and hence also denoted $CL_{passive}$. However in his case, the fluid which $CL_{passive}$ refers to is the brain ISF. In addition to symmetric transport across the BBB there is also asymmetric transport mediated by active transporters (Section 1.2.2). Active influx and efflux transport can also be described as net clearances composed of the sum of all active processes in one direction (CL_{influx} and CL_{efflux}) provided that the transporters are far from reaching their maximal capacity. Other processes that contribute to the elimination of drug from brain are metabolism (CL_{met}, Section 1.2.4) and bulk flow of brain interstitial fluid ($CL_{bulkflow}$, Section 1.2.3). Among all these clearance parameters $CL_{bulkflow}$ is unique in that it actually represents a physical flow i.e. the ISF bulk flow. Diffusion of drug from one location to another in the interstitial space is a random process that does not add or remove drug from brain. It is therefore not considered in the model. Diffusion of drug to and from CSF to adjacent brain tissue is ignored although such models have been constructed [30]. For simplicity, the unbound drug concentration in plasma ($C_{u,p}$) is here considered as a fix value to reflect continuous infusion of drug. To complete

the parameterization of the model a volume is ascribed to a single brain compartment. This is the $V_{u,brain}$ introduced in Section 1.2.5.

The model which is represented as boxes and arrows in Fig. 4 is also described by a single differential equation (Eq. 2). This equation describes how the rate of change in $C_{u,brainISF}$ ($dC_{u,brainISF}/dt$) depends on the simultaneous effects of the different transport processes. Positive and negative terms represent processes that take drug into the brain or remove drug from the brain, respectively. All terms are products of the clearance parameter and the unbound drug concentration in the fluid which is referred to i.e. $C_{u,p}$ for transport into the brain and $C_{u,brainISF}$ for elimination from the brain.

$$V_{u,brain} \times \frac{dC_{u,brainISF}}{dt} = C_{u,p} \times \left(CL_{passive} + CL_{\inf lux}\right) - C_{u,brainISF} \times \left(CL_{passive} + CL_{efflux} + CL_{met} + CL_{bulkflow}\right) \quad (2)$$

The model can be used to analyze the influence of different processes on $C_{u,brainISF}$, and its relation to $C_{u,p}$ over time. Since $C_{u,brainISF}$ and $C_{u,p}$ are the drivers for central and peripheral drug effects respectively, it is of immediate interest to determine the ratio of $C_{u,brainISF}$ to $C_{u,p}$ i.e. the unbound brain-to-plasma concentration ratio, $K_{p,uu,brain}$ [31]. As would be predicted by the model (Eq. 2), $K_{p,uu,brain}$ is time-dependent. The value for $K_{p,uu,brain}$ is small shortly after a given dose because the drug has not yet been allowed enough time to reach significant $C_{u,brainISF}$. At later time-points the value for $K_{p,uu,brain}$ is higher. However, since most drugs are given repeatedly during shorter or longer time-periods, the time-averaged value for $K_{p,uu,brain}$ i.e. the steady-state value is of particular interest. At steady-state there is no net movement of drug across the BBB i.e. $dC_{u,brainISF}/dt$ is zero. Eq. 2 can then be rearranged to explicitly express $K_{p,uu,brain}$:

$$K_{p,uu,brain} = \frac{C_{u,brainISF}}{C_{u,p}} = \frac{CL_{passive} + CL_{\inf lux}}{CL_{passive} + CL_{efflux} + CL_{met} + CL_{bulkflow}} \quad (3)$$

A number of important and useful points can be inferred from this relationship. The most obvious one is perhaps that $V_{u,brain}$ is no longer present. This means, for example, that increased binding of drug in brain tissue does not result in reduced average unbound drug concentrations. Counter-intuitive as this may be, it illustrates the power of using a holistic approach to the problem. The contribution of the various parameters to $K_{p,uu,brain}$ can also be evaluated. Beginning with the ISF bulk flow, the physiological value for $CL_{bulkflow}$ (Section 1.2.3) is much smaller than the sum of other elimination clearances for compounds with drug-like properties. Not even for the large and highly hydrophilic morphine-3-glucuronide does the ISF bulk flow account for more than 25 % of its elimination [32]. $CL_{bulkflow}$ can accordingly

be ignored in the denominator of Eq. 3, and the influence of ISF bulk flow be ruled out with the help of the model. Provided that the physiological magnitude of ISF bulk has not been greatly underestimated, it can also be inferred that optimization of drug delivery to the brain cannot rely on alterations of passive permeability alone, as can be done for optimizing oral drug absorption.

CL_{met} can be generally assumed to be small (Section 1.2.4), however in case it is not, it will be seen as a contributor to CL_{efflux}. Further, if there is no active influx or active efflux of a particular drug (something that cannot be generally assumed), $K_{p,uu,brain}$ becomes unity and the unbound drug concentration is the same in the brain and blood. Hence, the physical tightness of the BBB would not have been "value for money" had it not been for asymmetric *active* carrier-mediated transport. Finally, it is also seen that $K_{p,uu,brain}$ is greater than unity if CL_{influx} dominates over $CL_{passive}$ and CL_{efflux}, and that $K_{p,uu,brain}$ is smaller than unity when CL_{efflux} dominates over $CL_{passive}$ and CL_{influx} [33].

A model-based and quantitative analysis provided by Takasawa et al. [30], showed negligible contribution of brain-to-CSF diffusion for zidovudine and didanosine in rats. It may however not be possible to generalize these findings for all drugs since the contribution is dependent on several drug specific processes.

1.3 Methodologies for measurement of BBB transport

A substantial number of methodologies are available for the study of drug transport across the BBB in experimental animals. These *in vivo* methods can be grossly divided into two groups: 1) methods that measure the *rate* of drug transport and 2) methods measure the *extent* of drug transport across the BBB [34].

1.3.1 Rate of BBB transport

Methods that measure the rate of transport into brain include the intravenous injection technique [35], the *in situ* brain perfusion technique [36], and the carotid artery single injection technique [37] also known as the Brain Uptake Index. The readout of these methods is the BBB uptake clearance CL_{in}. By reference to the model (Eq. 3), CL_{in} is the sum of passive influx ($CL_{passive}$) and active influx (CL_{influx}). In reality, however, efflux transporters are known to hinder influx in addition to enhancing efflux [38].

Measurements of the rate of elimination from the brain are less common. The most well-known method is the intra-cerebral microinjection technique known as the Brain Efflux Index [39]. This method gives a value of the ef-

flux clearance (CL_{out}), which describes the combined effect of all processes that eliminate drug from brain i.e. passive and active efflux ($CL_{passive}$, CL_{efflux}) as well as metabolism (CL_{met}) and elimination by ISF bulk flow ($CL_{bulkflow}$).

The greatest value of the abovementioned methods is the possibility to delineate and study individual mechanisms of BBB transport such as the contribution of particular transporters [34].

1.3.2 Extent of BBB transport

As discussed above, the exposure of the brain to unbound drug is of highest importance for the pharmacology of the drug and thus its clinical use. Brain exposure as described by $K_{p,uu,brain}$ is a measure of the extent of BBB transport. By and large, the present thesis work was prompted by the lack of efficient methods to determine $K_{p,uu,brain}$ in animals. In order to determine $K_{p,uu,brain}$, $C_{u,brainISF}$ as well as $C_{u,p}$ need to be measured or estimated at steady-state during continuous infusion of drug (Eq. 4). An equivalent approach is to measure $C_{u,brainISF}$ and $C_{u,p}$ at multiple time-points following a single dose and calculate the ratio of respective area under the concentration-time curve ($AUC_{u,brainISF}$ and $AUC_{u,p}$):

$$K_{p,uu,brain} = \frac{C_{u,brainISF}}{C_{u,p}} = \frac{AUC_{u,brainISF}}{AUC_{u,p}} \quad (4)$$

1.3.2.1 Microdialysis

Methods for the study of BBB transport have been available in some form since the late 19th century when the BBB was first described. However, it was only with the continued development of the microdialysis technique in the 1990s that it became possible to actually quantify the unbound drug in the brain [40-42]. Using this technique both unbound drug and endogenous neurotransmitters are dialysed through a small semi-permeable dialysis membrane on a probe. The probe, which is surgically implanted in a brain region, is continuously perfused with a physiologic buffer solution allowing fractions of dialysate to be collected for drug analysis. Due to the continuous perfusion, the perfusate and brain ISF cannot be assumed to be in equilibrium. It is therefore necessary to determine the relationship between the unbound drug concentration in the ISF surrounding the probe and the dialysate concentration, i.e. to determine the recovery of the probe. This estimated probe recovery is then used to back-calculate $C_{u,brainISF}$ from the measured dialysate concentration. There are several different approaches to estimating probe recovery, many of which utilizes retrodialysis in some form i.e. the inclusion of the drug or a calibrator in the perfusion fluid to determine the

loss through the probe. Theory has it that the recovery by loss is equal to recovery by gain [43]. This principle is generally confirmed experimentally *in vitro* prior to *in vivo* experiments. A typical recovery value for a standard brain probe is ~10-20%. Recently, ultra-slow microdialysis with nearly 100 % recovery has been developed in order to circumvent the issue of estimating probe recovery. The extent of BBB transport ($K_{p,uu,brain}$) is determined by comparison with $C_{u,p}$ measured with another probe placed in a large blood vessel or by other techniques.

There are several advantages of using microdialysis in addition to measuring unbound drug. These include the multiple samples obtained over time in the same animal, which not only limits the use of animals but also allows both rate (CL_{in} and CL_{out}) and extent ($K_{p,uu,brain}$) to be measured. The limitations include various technical challenges such as advanced animal surgery, adsorption of lipophilic drugs to the tubing or probe membrane and the necessity to determine probe recovery. Arguments have been put forth that the BBB is damaged at the site of probe insertion [44], however studies show that the BBB has effectively recovered within 24 hours of the implantation [45]. There is also good agreement of CL_{in} values determined by microdialysis and other methods [33].

While the integrity of the BBB is likely to remain a matter of debate, it is noted that the microdialysis has been instrumental for the development of and recognition of the $K_{p,uu,brain}$ concept. Still today there is no other method of measuring $C_{u,brainISF}$ or $K_{p,uu,brain}$ exclusively *in vivo*.

1.3.2.2 Brain tissue sampling

In strong contrast to the delicate microdialysis method, brain tissue sampling approaches the extent of BBB transport by asking: "how much drug is there?" The measured entity is the amount of drug in brain (A_{brain}) i.e. the total brain concentration. Comparison is generally made with the total plasma concentration (C_p) to calculate the total brain-to-plasma concentration ratio $K_{p,brain}$ also known as BB or the logarithm thereof (logBB).

$$K_{p,brain} = BB = \frac{A_{brain}}{C_p} \tag{5}$$

It is obvious that it is difficult to interpret an amount of drug inside the cranium in terms of $C_{u,brainISF}$. Still, brain tissue sampling has been the most common practice in drug industry to assess the extent of BBB transport. Likewise, logBB remains commonly used for construction of various computational prediction models (see Section 1.4). The brain ISF in which we want know the unbound drug concentration only represents 20 % of the brain sample, the remaining 80 % being brain cells. Depending on the extent of drug uptake and binding inside cells, virtually any value of A_{brain} can oc-

cur for a given value of $C_{u,brainISF}$. Again, more non-specifically drug bound in brain cells is not reflective of unrestricted BBB transport, nor does it mean lower unbound drug concentration at extracellular or intracellular target sites. Hence it cannot be considered relevant to measure A_{brain} or $K_{p,brain}$ in isolation.

1.3.2.3 Combined *in vivo* tissue sampling and *in vitro* $V_{u,brain}$ measurement

Since $V_{u,brain}$ is the drug-specific proportionality constant between $C_{u,brainISF}$ and A_{brain} (Eq. 1) it should be possible to convert any measured value of A_{brain} to $C_{u,brainISF}$ by knowing the value of $V_{u,brain}$. It has been proposed that $V_{u,brain}$ can be determined *in vitro* using uptake studies in brain slices [39] as well as by measuring the unbound fraction in homogenized brain tissue ($f_{u,brain}$) using equilibrium dialysis [46, 47]. $C_{u,brainISF}$, and hence also $K_{p,uu,brain}$, is calculated by dividing A_{brain} by $V_{u,brain}$ measured in slices (Eq. 6) or by multiplying by the homogenate $f_{u,brain}$ (Eq. 7). $C_{u,p}$ is generally determined by multiplying the measured C_p by the unbound fraction in plasma ($f_{u,p}$), which is determined by equilibrium dialysis.

$$K_{p,uu,brain} = \frac{A_{brain}}{C_p \times V_{u,brain} \times f_{u,p}} = \frac{K_{p,brain}}{V_{u,brain} \times f_{u,p}} \quad (6)$$

$$K_{p,uu,brain} = \frac{A_{brain} \times f_{u,brain}}{C_p \times f_{u,p}} = K_{p,brain} \times \frac{f_{u,brain}}{f_{u,p}} \quad (7)$$

The methodology of combining standard brain tissue sampling techniques with simple *in vitro* estimates of $V_{u,brain}$ or $f_{u,brain}$ has sufficient throughput for broad implementation in drug discovery programs. The core question is whether the slice or homogenate method measures $V_{u,brain}$ or $f_{u,brain}$ *in vitro* such that a non-biased value for $C_{u,brainISF}$ results when combining with A_{brain} measured *in vivo*. This issue is assessed in Paper I of this thesis.

1.3.2.4 Correction for drug in residual blood

Whether sampling of brain tissue is done to measure the rate or extent of BBB transport, an inherent difficulty is the amount of drug in the residual blood of brain vasculature. This drug has not crossed the BBB and must be corrected for in order to obtain a value for A_{brain} that exclusively represents drug in brain tissue. The correction is normally done by subtracting the amount in residual blood calculated as the product of the plasma concentration and estimated volume of brain residual blood [48, 49]. The vascular volume in the brain is around 3 % in a live animal. For drugs with very small A_{brain} relative to C_p (small $K_{p,brain}$), the estimated A_{brain} can become very im-

precise or even negative. The problem is further complicated by the different composition of brain capillary residual blood compared to arterial blood in terms of hematocrit etc [50]. The reason for the different composition may include selective draining of red blood cells when the blood pressure falls to zero, or the presence of microdomains in the capillary network that are not large enough to accommodate blood cells or plasma proteins. The issue of correction for drug in residual blood is specifically addressed in Paper III where a drug-specific correction model for residual blood was proposed.

1.3.2.5 CSF sampling

Notwithstanding the intricacies of brain anatomy and physiology it is sometimes assumed that the CSF drug concentration (C_{CSF}) is equal to $C_{u,brainISF}$. It has therefore been relatively common to use sampling of CSF to assess drug exposure at central target sites both in experimental animals and in humans. Sampling of CSF can be done at various sites: in the ventricles via permanent catheters, by puncturing the occipital membrane of *cisterna magna* or by puncturing the lumbar membrane, which is the common procedure in humans. In analogy to $K_{p,uu,brain}$, the unbound CSF-to-plasma concentration ratio $K_{p,uu,CSF}$ can be estimated (Eq. 8) where $C_{u,CSF}$ represents the unbound drug concentration in CSF. Due to the very low protein concentration in CSF there is very little binding of drug and hence C_{CSF} can in most instances be directly used as an approximation of $C_{u,CSF}$.

$$K_{p,uu,CSF} = \frac{C_{u,CSF}}{C_{u,p}} \approx \frac{C_{CSF}}{C_{u,p}} \tag{8}$$

1.3.3 *In vitro* methods

Various *in vitro* approaches have been developed for the study of BBB transport [51, 52], including assays of pure passive permeability i.e. PAMPA [53], cell-culture models using primary brain endothelial cells, immortalized cell-lines of brain endothelial cells as well as cell culture models of other origin than the brain, i.e. CACO-2, MDCK and LC-PK1 cells.

A distinction is made between *in vitro* methods that measure the rate and extent of BBB transport, just as was done for the *in vivo* methods. *In vitro* BBB models are typically used to measure the rate of transport, i.e. BBB permeability. The extent of transport can principally also be assessed *in vitro* however this requires that the permeability in both directions is measured. The extent of BBB transport is expressed as the ratio of the two permeability values, i.e. the *efflux ratio*. There is a direct analogy between the *in vitro* efflux ratio and the *in vivo* $K_{p,uu,brain}$, which is the ratio of CL_{in} and CL_{out}. So far, the results from *in vitro* models with brain endothelial cells have been rather disappointing in that only very modest efflux ratios have been re-

ported. In terms of describing asymmetric drug transport Pgp-transfected cell-lines such as MDR1-MDCK seem to be superior [34]. The merit of *in vitro* models is that the biology and mechanisms of drug transport can be studied in detail. Most importantly, *in vitro* methods present the only opportunity to study BBB transport with human material in drug discovery.

1.4 Methodologies for prediction of brain exposure

Being able to *measure* drug exposure in the brain is obviously of great value in drug discovery programs since it helps to understand the pharmacology of the drug and also to guide the selection of compounds for further development. *In vitro* models of the BBB also have a place here by acting as a filter with higher throughput than animal experiments. However, it is of yet greater value if one would be able to tell beforehand i.e. *predict* which molecules will have the appropriate level of brain exposure before the compounds are even synthesized. The key element of such computational *in silico* models is to characterize the relationship between the chemical structure of the drug and the level of brain exposure. The goal, which is to *design* brain exposure into the structure of the drug, also requires that the prediction model is not more complicated than to allow the chemist to interpret the model in terms of favorable directions.

1.4.1 Computational model development

The procedure for developing predictive computational models for e.g. brain exposure can be divided into five general steps: 1) selecting a relevant set of drug molecules; 2) generating experimental data for the drug property of interest; 3) describing the chemical structure of the molecules in terms of numerical descriptor values; 4) relating the structural description to the experimental data using a mathematical relationship; and 5) validating the predictivity of the model [54].

1.4.1.1 Compound selection

The selection of a *training-set* of compounds on which to build the relationship between brain exposure and molecular structure is not an arbitrary choice, since it will define the *applicability domain* of the model. The desired applicability domain can be larger e.g. to encompass drugs in general (global models) or small to encompass only structures that are relevant to a particular drug discovery program (local models). A higher level of predictivity is expected from local models than from global models though it comes at the expense of a more restricted applicability domain. Regardless of whether global or local models are considered, one should strive for a structurally diverse selection within the domain.

1.4.1.2 Molecular descriptors

Molecular structures need to be translated in to numerical representations before a mathematical relationship can be derived with the measured drug property. This is done by *molecular descriptors* encoding various properties of the molecule. There are several sets of descriptors which are associated with the different computational approaches or software. For prediction of BBB transport, however, standard physicochemical descriptors have been commonly used. Physicochemical descriptors provide information about the molecular size, shape, lipid solubility (lipophilicity) as well as information on the hydrogen bonding potential of the drug. Acid-base properties i.e. proton dissociation constants (pKa) can also be predicted from the structure and used to classify drugs as neutral, positively or negatively charged at physiological pH.

1.4.1.3 Generation of experimental data

This step is often considered the most costly and time-demanding step of model development. There is consequently always a risk of using inadequate experimental methods or not applying sufficiently stringent criteria for inclusion of experimental data from literature. It is well known that good quality data are a *conditio sine qua non*, an absolutely essential condition. A prediction model can never make better predictions than the experimental data used for its generation.

1.4.1.4 Relating experimental data to molecular descriptors

Given the influence of the drug chemistry in the various aspects of drug disposition in the brain it is not surprising to find relationships between experimental measurements and molecular descriptors. There are several mathematical or statistical modeling approaches that can be used in the process of describing these relationships. The simplest form would be to look at the correlation between the measured drug property and individual molecular descriptors. If a strong relationship is found (linear or not), the equation describing the relationship could be used as a computational prediction model for future compounds. If a strong relationship cannot be seen with any one descriptor, it is possible that several descriptors can give a better prediction when combined. The modeling method used in this thesis (Paper IV) is *partial least squares projection to latent structures* (PLS) [55]. By this method of modeling, a larger number of molecular descriptors can be reduced to a smaller number of latent super-variables or *principal components*, which are then related to experimental data. Advantages of using PLS include that descriptors that are irrelevant to the problem are handled as well as closely related (correlated) descriptors. PLS models are also easily interpreted in terms of how the molecular properties could be changed. A major drawback

is PLS being a linear method which cannot detect and describe non-linear relationships, which are abundant in nature.

1.4.1.5 Validation of the model

Before a computational prediction model can be taken into practice it must be validated. While the coefficient of determination (R^2) describes the correlation between observed and predicted values for the training-set, it cannot be taken for granted that the predictivity is equally good for drugs not used for training the model. In fact, R^2 should never be used to compare prediction models or be expected to reflect the real model predictivity for new compounds. Cross-validation or *leave-many-out* is a method for validating a model [56]. By dividing the compounds in groups, a model can be generated based on all groups but one, for which the values are instead predicted. The procedure is repeated until all groups have been withheld from the model and predicted. The cross-validated coefficient of determination (Q^2) is generally the first method of validating a PLS model, and is used continuously to assess the predictivity of rivaling models. Unfortunately, a high value for Q^2 is neither a guarantee for a predictive model. The only way to really validate a prediction model is to use an external *test-set* of compounds which have not at all been used in the training of the model. Failure of a high Q^2 model to satisfactorily predict compounds in a test-set indicates that there are unresolved issues with defining the applicability domain of the model. This highlights the importance of the compound selection procedure which, if made appropriately for the problem at hand, increases the chances of obtaining a model that is fit-for-purpose. As a final note, there are no computational tools to indicate the validity or relevance of the modeled experimental data.

1.4.2 Overview of BBB prediction models

The era of computational modeling of BBB transport began in 1980 when Levin [10] observed a strong relationship between the BBB permeability (CL_{in}) and the octanol-water partitioning coefficient (LogP) for a set of 27 compounds. Interestingly, four compounds with molecular weight greater than 400 Dalton were excluded from the analysis since they were considered "extremely restricted" owing to their size. In retrospect it is realized that these were substrates of Pgp. It was, however, concluded that there exists a molecular weight cutoff for "significant BBB passage". A relationship between descriptors of lipophilicity and logBB was also found by Young et al. in 1988 [57] for a set of 20 antihistamines. Since then, the public dataset of logBB values has expanded well over a hundred compounds, and several computational approaches have been used by different groups [58-63]. These studies taken together [64] indicate that brain penetration as measured by logBB is negatively correlated to descriptors of hydrogen bonding e.g. the

number of hydrogen bond donors (HBD), acceptors (HBA) or polar molecular surface area (PSA). A positive correlation with logBB is seen for descriptors related to lipophilicity such as LogP. Furthermore, acids having a negative charge at physiological pH generally have lower logBB than do basic drug with a net positive charge. The underlying mechanisms of these findings are identified and discussed in Paper IV.

In order to remedy the relatively limited availability of logBB values, larger datasets have been created by classifying marketed or investigational drugs as CNS active (CNS+) or inactive (CNS-) according to the presence or lack of central drug effects or side effects. The underlying assumption of this approach is that CNS+ drugs "cross" the BBB whereas CNS- drugs do not. This is obviously correct for all CNS+ drugs but the lack of CNS effects of CNS- drugs can arguably have different backgrounds. Values of logBB have also been added to these datasets by using arbitrary cutoff values for classification as CNS+ or CNS-. Nevertheless, the prediction accuracy of this kind of classification approaches has been fairly good especially for CNS+ drugs [64]. A justified objection to categorical modeling is that brain exposure is a continuous variable by nature, and strictly speaking, CNS- drugs do not exist since all drugs enter the brain to some extent.

Much of what is considered to be known about BBB has actually been learnt from the related field of intestinal drug absorption. Palm et al. [65] demonstrated that orally administered drugs should not exceed a polar molecular surface area (PSA) greater than 120 $Å^2$. Inspired by this work, Kelder et al. [66] published a prediction model for logBB based on PSA together with an analysis showing that the majority of CNS+ drugs have PSA 60 $Å^2$ or less. This has given rise to the perception that the BBB is "tighter" than the intestinal membrane, and that a window of PSA exists for orally absorbed but CNS inactive drugs. Principles derived for oral drug absorption should not be directly applied to the BBB, since the BBB represents an altogether different system. For oral drug absorption, the rate of membrane transport is crucial, since there is a limited intestinal transit time [34]. In contrast there is no definite time limit for the BBB transport as the drug continuously circulates in blood, during a repeated dosing situation. This makes the net rate of inward membrane transport (CL_{in}) much less important for the BBB.

1.5 Translation to humans

A commonly used notion is that the BBB is "conserved" between mammalian species. According to such an assumption it would be feasible to directly translate data on BBB transport in preclinical species to man. While the overall architecture of BBB is conserved, and perhaps also most of its physical aspects, current understanding of the pivotal role of drug transporters cast

doubt on this assumption. Human transporters generally have one or more *orthologous* transporter counterpart expressed in other species. For example, the human drug transporting Pgp is encoded by a single gene and protein (MDR1) whereas the mouse has two versions (mdr1a and mdr1b). The amino acid sequence of orthologous transporters is never exactly the same, which has potential effects on the transport efficiency for the particular drug. Furthermore, the expression level i.e. the abundance of each transporter may differ between species.

The assumption of a species-conserved BBB is particularly critical for decision making in drug discovery as new compounds enter clinical trials largely based on animal data. Approaches for scaling or translating animal or *in vitro* BBB data to humans are not as well developed as those of e.g. drug elimination by the liver. This is, in part, related to the difficulties of establishing human *in vitro* BBB models. There are also limited possibilities of actually validating such models since there are essentially no solid data available on brain exposure in humans.

Sampling of CSF has been a relatively commonly used clinical procedure, however, the applicability of CSF concentrations has been rightfully questioned [67] since CSF represents a different compartment than the brain ISF. Imaging by Positron Emission Tomography (PET) allows the $K_{p,brain}$ of the labeled drugs to be determined in humans, but this has been done only for a limited number of drugs [68]. In Paper IV, literature data on drug concentrations in CSF are compared with corresponding measurements in rats.

2 Aims of the thesis

The general objective of this thesis was to develop an efficient methodology for measurement of unbound drug exposure in the brain and to explore the relationships with the chemical structure of the drug.

The specific aims were:

- To verify by comparing with *in vivo* microdialysis that intra-brain drug distribution ($V_{u,brain}$) can be quantified *in vitro* using brain slice or homogenate methods (Paper I).

- To establish experimental conditions of the brain slice method such that it can be applied for drugs with various properties in a high-throughput manner (Paper II).

- To develop a correction model for drug in residual blood of brain tissue samples so as to improve the accuracy of brain exposure measurements (Paper III).

- To apply the methodology developed in Papers I-III for the generation of a novel dataset of the unbound brain-to-plasma and CSF-to-plasma concentration ratios, $K_{p,uu,brain}$ and $K_{p,uu,CSF}$ (Paper IV).

- To attempt developing computational prediction models for $K_{p,uu,brain}$ and relate to previous prediction models based on measurement of logBB (Paper IV).

- To investigate the relationship between $K_{p,uu,brain}$ and $K_{p,uu,CSF}$ to evaluate the use of $K_{p,uu,CSF}$ as a surrogate for $K_{p,uu,brain}$ (Papers III-IV).

- To approach the issue of translating rat $K_{p,uu,brain}$ and its relationships with drug structure to the human, by comparing rat $K_{p,uu,CSF}$ with compiled literature values for $K_{p,uu,CSF}$ in humans (Paper IV).

3 Methods

3.1 Animals

Male and female Sprague-Dawley rats were obtained from Harlan (Horst, The Netherlands). Male Dunkin Hartley guinea pigs were obtained from Lidköpings Kaninfarm (Lidköping, Sweden). All animals were acclimatized for a minimum of 5 days at 22°C during a 12-hour light-dark cycle with free access to food and water. Ethics approvals were obtained from the Animal Ethics Committee of Göteborg University for Paper I (346-2002, 412-2005), Paper II (412-2005), Paper III (169-2006, 221-2008) and Paper IV (412-2005, 169-2006, 221-2008). Female rats (230-280 g) were used for *in vivo* microdialysis in Paper I. Guinea pigs were used for *in vitro* brain slice and homogenate experiments with cetirizine in Paper I. Male rats (250-400 g) were used in all other *in vitro* and *in vivo* experiments of Papers I-IV.

3.2 Animal surgery

Isoflurane inhalation anesthesia (FORENE®, Abbot Scandinavia AB, Solna Sweden) was used in surgical procedures throughout Papers I-IV. Rats were prepared for infusion experiments (Papers III-IV) by catheterization of the left femoral vein for drug administration using a PE-10 cannula fused with PE-50 tubing. The rats were given ketoprofen as adjuvant analgesics (Romefen® Vet, Merial, Lyon, France) and were rehydrated (Rehydrex®) and allowed a post-operative recovery period of 24 hours prior to the experiment.

3.3 Compound selection

Drugs were selected as model compounds for the development of experimental methods (Papers I-III) and computational methods (Paper IV). Since the general aim was to develop methods that are applicable to a wide range, if not all, drug-like small molecules, a diverse and representative selection was required.

The selection of compounds for Paper I was dictated by the availability of microdialysis data in literature on $V_{u,brain}$. The set of 14 drugs or drug metabolites that were included in the study was biased towards more hydrophilic

compounds due to the fact that lipophilic compounds are difficult or impossible to study with microdialysis. The bias was partially remedied by inclusion of one moderately lipophilic compound (CP-122721) for which $V_{u,brain}$ could be determined in new microdialysis experiments.

In Paper II, which aimed to optimize the slice method, six drugs were used as model compounds based on prior knowledge of their mechanisms of distribution. Gabapentin was chosen based on its active uptake into brain cells. Neutral (diazepam and rimonabant), basic (thioridazine and paroxetine) as well as acidic (indomethacin) drugs were represented since distribution in brain slices was found to be pH dependent (Paper I). Special care was taken to include lipophilic compounds with potentially high $V_{u,brain}$ (paroxetine, thioridazine and rimonabant) since these would not be possible to study with microdialysis and since drugs with high $V_{u,brain}$ showed to be difficult also in the preliminary setup of the slice method.

Paper III aimed at improving the correction for drug in the residual blood of brain tissue samples. The three selected model drugs (indomethacin, loperamide and moxalactam) were known beforehand to be potentially sensitive to the correction due to having low values of $K_{p,brain}$ (see Section 1.3.2.4). Furthermore, they exhibited widely different patterns of binding in the brain ($V_{u,brain}$) relative to the respective binding in plasma ($f_{u,p}$). This was to illustrate the inter-relationship between binding in the brain vs. plasma and the problem of correcting for drug in residual blood.

The aim of Paper IV was to generate a large dataset of $K_{p,uu,brain}$ and $K_{p,uu,CSF}$ and use this to develop computational prediction model for $K_{p,uu,brain}$ and assess the applicability to human by comparing rat and human $K_{p,uu,CSF}$. For the compound selection it was therefore needed to consider the availability of literature values of $K_{p,uu,CSF}$ in human patients. A representative selection was, however, required since *global* computational prediction models were desired since they are applicable to the entire chemical drug space. To meet both these criteria, a literature review of human CSF data provided by Shen et al. [8], was used as starting point. This CSF dataset contained clinical data on drug concentrations in the CSF for 92 drugs from 5 different therapeutic areas. An independent data set of 24 diverse drugs [69] represented the range of chemical structural space for drugs on the Swedish market (diverse data set). In order to ensure a representative selection of drugs from the CSF data set the diverse data set was used as a template as follows. Molecular descriptors (Section 1.4.1.4) were calculated for all compounds. A principal component analysis (PCA) using Simca-P+ [70] was performed for the 24 drugs of the diverse data set. The 92 drugs of the CSF data set were projected onto this PCA, and 36 drugs were initially selected from the CSF dataset according to the resulting scores. Drugs with significant bioanalytical challenges were later replaced by similar drugs. Drugs of particular interest for the BBB were added even if they were not included in the CSF dataset. The final data set consisted of 43 compounds, with human

CSF data available for 32 of the 43 compounds. Fig. 5 shows the distribution of the selected compounds in comparison to the diverse data set and the CSF data set in the PCA score plot.

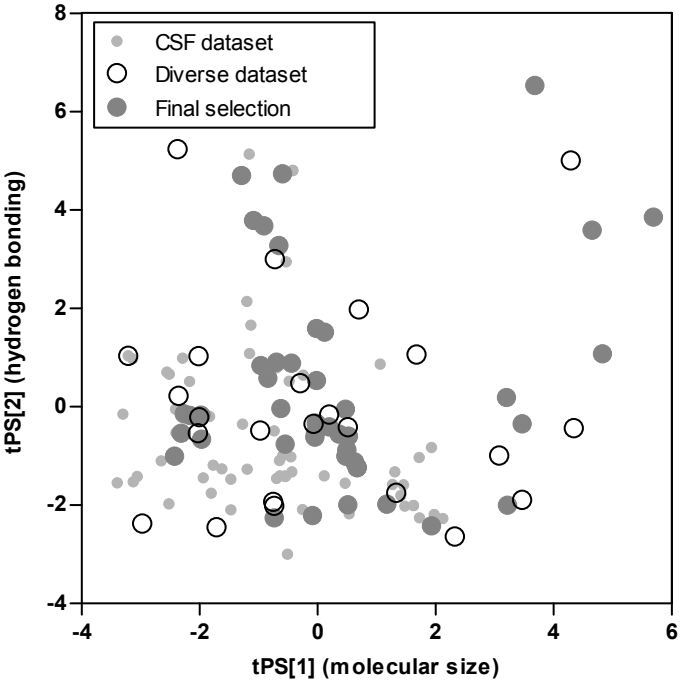

Figure 5. PCA score plot of the CSF dataset, the diverse dataset and the selected drugs. Principal components 1 (tPS[1]) and 2 (tPS[2]) represent the molecular descriptor related to molecular size and hydrogen bonding (polarity), respectively.

3.4 Determination of intra-brain distribution, $V_{u,brain}$

In Paper I, the *in vitro* brain slice and brain homogenate methods for measurement of $V_{u,brain}$ were compared with the *in vivo* microdialysis method. Each method is presented below.

3.4.1 *In vivo* microdialysis

The main source of microdialysis data on $V_{u,brain}$ in Paper I was literature reports. In these studies the $V_{u,brain}$ determined by microdialysis ($V_{u,brain,MD}$) was calculated by dividing A_{brain} measured by conventional brain tissue sampling by $C_{u,brainISF}$ measured by microdialysis in the same animal (Eq. 9).

$$V_{u,brain\,(MD)} = \frac{A_{brain}}{C_{u,brainISF}} \tag{9}$$

3.4.2 *In vitro* brain slice method

The brain slice method which was adapted from the work of Kakee et al. [39], was used in a preliminary setup in Paper I. The following describes the optimized setup which was developed in Paper II and implemented in Papers III-IV.

Six 300-µm slices (see cover art) from a drug-naïve rat were cut using a DTK-Zero1 Microslicer (Dosaka, Kyoto, Japan) and transferred into a ∅80-mm glass dish containing 15 ml of buffer plus up to 10 drugs to be studied at a concentration of each 100 nM. The tray was placed in a humidified and oxygenated box inside a Forma Orbital Shaker 420 (Thermo Fisher Scientific, Waltham, MA) set at 35°C. After 5 hours incubation the slices were dried on filter paper and weighed in a 2-ml Eppendorf tube (~33 mg). The slices were individually homogenized in 9 volumes (w/v) of buffer with an ultrasonic probe (Sonifier 250; Branson Ultrasonics, Danbury, CT). The buffer was sampled directly from the dish. $V_{u,brain}$ determined in brain slices ($V_{u,brain(s)}$) was calculated according to

$$V_{u,brain(s)} = \frac{A_{slice} - V_i \times C_{buffer}}{C_{buffer}\left(1 - V_i\right)} \tag{10}$$

where A_{slice} and C_{buffer} are the amount of drug in the slice per gram and the concentration of drug in the buffer, respectively. V_i (milliliters per gram of slice) is the volume of buffer film that remains around the sampled slice because of incomplete absorption of buffer by the filter paper. V_i (0.094 ml/g_slice) was estimated using ^{14}C-inulin in a separate experiment.

3.4.3 *In vitro* brain homogenate binding method

Brain homogenate was prepared from the brains of drug-naïve rats in 3 volumes of a 122 mM phosphate buffer (pH 7.4). The studied drugs were added to the homogenate and equilibrium dialysis of homogenate and buffer was performed in triplicate for 16 h at 37°C in 1 ml Plexiglas cells mounted with a 5-kDa cutoff Diachema cellulose membrane (Dianorm GmbH, München, Germany). The fraction of unbound drug in diluted brain homogenate, $f_{u,hD}$, i.e. the buffer-to-homogenate concentration ratio, was used to calculate $f_{u,brain}$, while also taking into account the dilution (D) associated with homogenate preparation (Eq. 11) [46]. The inverse of $f_{u,brain}$ ($V_{u,brain(h)}$) was used to

express the quantity on the $V_{u,brain}$ scale to facilitate comparison with microdialysis and brain slices (Eq. 12).

$$f_{u,brain} = \frac{1}{1 + D\left(\frac{1}{f_{u,hD}} - 1\right)} \tag{11}$$

$$V_{u,brain(h)} = \frac{1}{f_{u,brain}} \tag{12}$$

3.5 Measurement of $K_{p,uu,brain}$ and $K_{p,uu,CSF}$ *in vivo*

The work around developing the brain slice method for measurement of $V_{u,brain}$ (Papers I-II) enabled its application for generating a large rat-dataset of $K_{p,uu,brain}$ by combining with conventional brain tissue sampling. This combined approach, which is described below, is significantly faster as compared to microdialysis. As a potential surrogate for $K_{p,uu,brain}$, the unbound CSF-to-plasma ratio ($K_{p,uu,CSF}$) was determined in the same animals.

The drugs were administered in cassettes of two to three drugs as 4 h constant-rate intravenous infusions to approach steady state using an infusion flow rate of 1 (mL/kg)/h, corresponding to dosage rates of 2 (μmol/kg)/h for each drug. Each cassette was given to a separate group of rats. The vehicle used was saline or a 1:1:1 (w/w/w) mixture of dimethyl acetamide, tetraethylene glycol, and water. At the end of the infusion, the rats were anesthetized by inhalation of isoflurane. CSF (50 μL) was collected by puncturing the occipital membrane of *cisterna magna* using a fine needle connected to a cannula. The CSF sample was dispensed from the cannula into a 96-deep-well plate containing 5 μL of blank plasma, followed by rinsing three times with 50 μL of methyl tert-butyl ether/hexane (1:1) to minimize adsorption of lipophilic drugs to the walls of the catheter. Immediately after CSF sampling, a blood sample (~2 mL) was collected in a heparinized tube from the abdominal aorta, followed by immediate severing of the heart. The brain was removed, and a coronal section (6 mm) containing striatum was cut and divided into smaller pieces. A brain sample (350-375 mg) was transferred to an Eppendorf tube and homogenized in three volumes of deionized water using an ultrasonic probe.

The unbound fraction in plasma ($f_{u,p}$) was measured for each drug using an equilibrium dialysis method [71]. Pooled plasma from all rats, with each of the rats given a cassette of drugs, was divided into three to five aliquots of 200 μL and dialyzed overnight against 200 μL of phosphate buffer (122

mM). A buffer pH of 7.0 was used in order to offset an upward shift in pH during the dialysis, resulting in a final pH of 7.4.

The correction model for drug in residual blood, which was developed in Paper III was used in the determination of A_{brain}. A_{brain} was accordingly calculated from the total drug concentration in brain homogenate ($C_{brain,h}$) corrected for drug in the *effective plasma space* (V_{eff}) and the brain residual plasma water volume (V_{water}):

$$A_{brain} = \frac{C_{brain,h} - V_{eff} \times C_p}{1 - V_{water}} \tag{13}$$

V_{eff} is the apparent plasma distribution volume of drug in the brain and is dependent on $f_{u,p}$ of the drug. It has a value between the physical plasma water volume (V_{water}, 10.3 µl/g_brain) and the slightly smaller apparent brain distribution volume of plasma protein ($V_{protein}$, 7.99 µl/g_brain).

$$V_{eff} = f_{u,p} \times V_{water} + (1 - f_{u,p}) \times V_{protein} \tag{14}$$

Using the corrected A_{brain}, $K_{p,uu,brain}$ was calculated with Eq. 6. $K_{p,brain}$ i.e. logBB was calculated using Eq. 5.

$K_{p,uu,CSF}$ was calculated according to Eq. 15 after estimation of the unbound fraction in CSF ($f_{u,CSF}$) based on the albumin CSF-to-plasma concentration ratio of 0.003 [72] (Eq. 16).

$$K_{p,uu,CSF} = \frac{C_{u,CSF}}{C_{u,p}} = \frac{C_{CSF} \times f_{u,CSF}}{C_{u,p}} \tag{15}$$

$$f_{u,CSF} = \frac{1}{1 + 0.003\left(\frac{1}{f_{u,p}} - 1\right)} \tag{16}$$

3.6 Computational modeling

3.6.1 Molecular descriptors

The following molecular descriptors were calculated: ClogP, ACDLogP, ACDLogD7.4, molecular weight (MW) and volume (VOL), number of rings (RingCount) and rotatable bonds (RotBond), van der Waals nonpolar

(NPSA) and polar surface area (PSA), and the number of hydrogen bond donors (HBD) and acceptors (HBA) as defined by Lipinski. The pK_a of all drugs was measured experimentally using capillary electrophoresis and mass spectrometry [73]. The fraction of drug molecules that were un-ionized at pH 7.4 (LogUnionized) was calculated accordingly, and the drugs were classified as acid, base, neutral, or zwitterion according to the most abundant ion species at pH 7.4.

3.6.2 PLS modeling

To find relationships between brain exposure of the drug and the chemical structure, the PLS method was applied using Simca-P+ with default settings. PLS models for $K_{p,uu,brain}$ and $K_{p,brain}$ were developed on the basis of a training-set comprising the original experimental *in vivo* data obtained using the brain slice method for all 43 drugs. $K_{p,uu,brain}$, $K_{p,brain}$ and the fraction unionized were log transformed prior to model development. As an initial assessment of the importance of each variable, the linear coefficient of determination (R^2) was calculated between $\log K_{p,uu,brain}$ and $\log K_{p,brain}$ and each of the 16 variables. To start with, all 16 descriptors were used in the development of PLS models; however, a variable selection procedure was used, in which groups of descriptors that did not contain information relevant to the problem (i.e., noise) were removed in a stepwise manner. This was to optimize and simplify the models. Descriptors were excluded from the model based on the variable importance for projection score in Simca-P+. The predictive performance of the new model was assessed according to the cross-validated coefficient of correlation (Q^2). The variables were generally excluded up to the point where there was no improvement in Q^2 by further exclusion of variables.

3.7 Bioanalytical methods

3.7.1 Technical procedures

The amount of drug in the various sample matrices was quantified with reversed phase liquid chromatography and multiple reaction monitoring mass spectrometry (liquid chromatography-tandem mass spectrometry, LC-MS/MS) detection using Micromass (Waters, Manchester, UK) triple-quadrupole instruments equipped with electrospray. Gradient elution over 1-2 min with acetonitrile and 0.2% formic acid with a flow rate of 0.6 ml/min was used with various C18 columns. Mass transitions and detailed chromatographic conditions for each compound are given in the respective publication (Papers I-IV). Sample preparation was adapted for any compound-specific requirements but followed a general procedure: samples of plasma,

brain homogenate etc. as well as standards made in the appropriate sample matrix were added in aliquots of 50 µl to 96-deepwell plates (Nalgene Nunc International, Rochester, NY). Protein-precipitation was made by addition of 150 µl of ice-cold acetonitrile containing 0.2% formic acid. After 1 min of vortexing and 20 min of centrifugation at 4000 rpm (Rotanta/TR; Hettich, Tuttlingen, Germany) at 4°C, the supernatant was transferred to a new plate and appropriately diluted with 0.2% formic acid. Injections of 5 to 20 µl were made from this plate to the LC-MS/MS system.

3.7.2 Drug quantification

External calibration curves were used throughout Paper I and for quantification of all *in vivo* samples in Papers III-IV. Standards with at least five different concentrations were prepared from a serial dilution of drug in 50% acetonitrile and 0.2% formic acid by standard addition to the blank matrices in a 1:9 volume ratio. Linear or quadratic calibration curves were fitted to the instrument response (chromatographic peak areas) and used for drug quantification. Calibration curves with R^2 greater than 0.990 were considered acceptable.

Samples from *in vitro* assays e.g. brain slice experiments in Papers II-IV, brain homogenate experiments in Papers II-III and the plasma protein binding assay (Paper IV) were analyzed without the use of standards. In these assays there is little use to make an absolute quantification of drug since the results are anyway expressed as a ratio of two concentrations such as the concentration on either side of the dialysis membrane in the equilibrium dialysis assay. Therefore, the chromatographic peak areas in the respective matrix, e.g. plasma and buffer, were directly used for calculations. To ensure that the responses used in the calculations were within the linear response range of the mass spectrometer, additional dilutions (10- and 100-fold) of protein precipitated the samples were made in 37.5% acetonitrile with 0.2% formic acid. These dilutions were analyzed together with the un-diluted samples. Any effects of nonlinearity in response were minimized by choosing one of the three different analyzed dilutions (1-, 10-, or 100-fold) such that the peaks for e.g. plasma and buffer were of similar size for each compound. Before calculations, the peak areas were scaled back to undiluted samples by multiplying by the dilution factors 1, 10, or 100 as appropriate.

Radioactive isotopes were quantified using a Wallac WinSpectral 1414 liquid scintillation counter (Wallac, Turku, Finland) and an OptiPhase HiSafe 3 scintillation cocktail (Fisher Chemicals, Loughborough, UK). Homogenates of brain or brain slices were solubilized with 1 ml of Soluene-350 (PerkinElmer Life and Analytical Sciences, Boston, MA) and decolorized with 100 µl of hydrogen peroxide.

3.8 Statistical analysis

3.8.1 Method comparison using Altman and Bland analysis

In Paper I, the agreement with microdialysis $V_{u,brain}$ and $V_{u,brain}$ determined with the brain slice and homogenate methods, respectively, was evaluated according to the method of Altman and Bland [74, 75]. Since experimental variability appeared to be proportional to $V_{u,brain}$, i.e. the coefficient of variation was similar for compounds with very different $V_{u,brain}$, log-transformation of data was done. The significance of a mean difference (bias) was tested with Student´s *t* test. The agreement between methods was expressed as a 90% confidence interval ratio (CIR) around the observed antilogged mean difference (bias), which was calculated using the *t* distribution. Owing to the log-transformation of data, the 90% *confidence interval* is the antilogged mean difference *divided* by the 90% CIR to the mean difference *multiplied* by the 90% CIR.

3.8.2 Statistical modeling of variance components

In Paper II, the aim was to optimize the brain slice method and arrive at a standardized design scenario using which $V_{u,brain}$ is precisely determined with a minimum of work. This required the identification and quantification of the various sources of variability in the method. The potential sources of variability were the inter-day variability, the variability associated with using slices from different rats, the variability between slices and the analytical variability. Using the optimized experimental setup, the $V_{u,brain}$ was determined for six model compounds on three days, in six slices from six rats with duplicate analytical measurement on two different days. This dataset of 1296 $V_{u,brain}$ determinations (6 compounds × 3 days × 6 rats × 6 × slices × 2 analytical replicates) was analyzed using mixed modeling [76] to generate the contribution of the different sources of variability. These figures were subsequently used to simulate 95% CIRs of various design scenarios.

3.8.3 The propagation of error method

In Paper III, the statistics was addressed for the combined use of *in vivo* brain tissue sampling and *in vitro* brain slice method. By this combined approach (Section 1.3.2.3), $K_{p,uu,brain}$ is determined as a function of four measured variables namely A_{brain}, C_p, $V_{u,brain}$ and $f_{u,p}$. By the correction model for drug in residual blood A_{brain} was expanded to itself be a function of six variables. Hence, $K_{p,uu,brain}$ was expressed as a function of altogether nine variables, which are all estimated with some experimental variability. The propagation of error method [77] was used to assess the overall precision of $K_{p,uu,brain}$ determined for a particular compound as well as the contribution of

individual variables. This was to identify the weak spots of the methodology. Expressed in general terms, this statistical approach estimates the standard error of a function Y=f(X, Z, …) with the following formula:

$$s_y = \sqrt{\left(\frac{\partial Y}{\partial X}\right)^2 s_x^2 + \left(\frac{\partial Y}{\partial Z}\right)^2 s_z^2 + \ldots} \qquad (17)$$

where s_y, s_x and s_z are the standard errors of function Y and measurements X and Z, assuming zero covariance between variables. $\partial Y/\partial X$ and $\partial Y/\partial Z$ are the partial derivatives of function Y with regard to X and Z, respectively.

3.8.4 Statistical tools for computational modeling

In Paper IV, PLS was applied to the dataset of $K_{p,uu,brain}$ and $K_{p,brain}$ as described in Section 3.6.2. The primary statistical evaluation of the prediction models was the leave-many-out cross validated Q^2 also referred to as model predictivity (Section 1.4.1.5). Q^2 was automatically calculated by the software using seven cross-validation groups. The predictivity of the final models was further characterized by the root of mean squared error of prediction (RMSE) calculated as

$$RMSE = \sqrt{\frac{1}{n}\sum_{i=1}^{n}\left(y_{i,predicted} - y_{i,observed}\right)^2} \qquad (18)$$

where n is the number of observations and $y_{predicted}$ and $y_{observed}$ are the experimentally determined and predicted values respectively.

4 Results and discussion

4.1 Evaluation of *in vitro* measurements of $V_{u,brain}$

In Paper I, the *in vitro* brain slice and brain homogenate methods for measurement of intra-brain distribution ($V_{u,brain}$) were compared with corresponding measurements *in vivo* using microdialysis. This was to determine whether any one of the *in vitro* methods would be suitable to combine with conventional sampling of whole brain tissue to yield estimates of $C_{u,brainISF}$.

The 15 drugs included in the study exhibited a wide range of $V_{u,brain}$ values as determined using microdialysis. The morphine glucuronides M3G and M6G had values lower than unity (0.25 and 0.20 ml/g_brain respectively) indicating that they were predominantly distributed outside the brain cells in the ISF. At the other extreme the moderately lipophilic and basic drug CP-122721 had a 1000-fold higher $V_{u,brain}$ value (207 mL/g_brain) owing to extensive uptake and binding inside the cells.

The overall *in vivo* agreement of the slice and homogenate method was described by the 90% CIR. There was no evidence of overall bias for either method. As would be expected from the slice method being a more physiologic system, it also performed better according the much smaller CIR (2.95) compared to the CIR for the homogenate method (6.00). This is also illustrated in Fig. 6 where 14 and 10 out of the 15 drugs were within 3-fold of microdialysis values for the slice and homogenate method, respectively.

The better agreement of the slice method is well understood when considering the individual drugs in the study and the various mechanisms by which they distribute within the brain. Starting at the lower end by taking M3G as example; the preferential distribution outside cells is also seen in the brain slices as $V_{u,brain}$ having a value lower than unity (0.53 ml/g_brain). In contrast, the homogenate method gives a value close to unity (1.2 ml/g_brain) only indicating that there is little or no binding to tissue constituents. A $V_{u,brain}$ value at unity or above is inherent for the homogenate method since the intracellular and interstitial spaces are mixed in a homogenate. The viability and *in vivo* agreement of the brain slices is also seen by the active uptake of gabapentin, which in the absence of binding (homogenate $V_{u,brain}$ 1.05 ml/g_brain) results in $V_{u,brain}$ of 5.5 in microdialysis experiments and 4.0 in the slices. Moreover, there was a tendency for basic drugs to have higher $V_{u,brain}$ in the slices relative to the homogenate method. This is consis-

tent with the pH partition theory [78] and the lower intracellular pH of brain tissue [5].

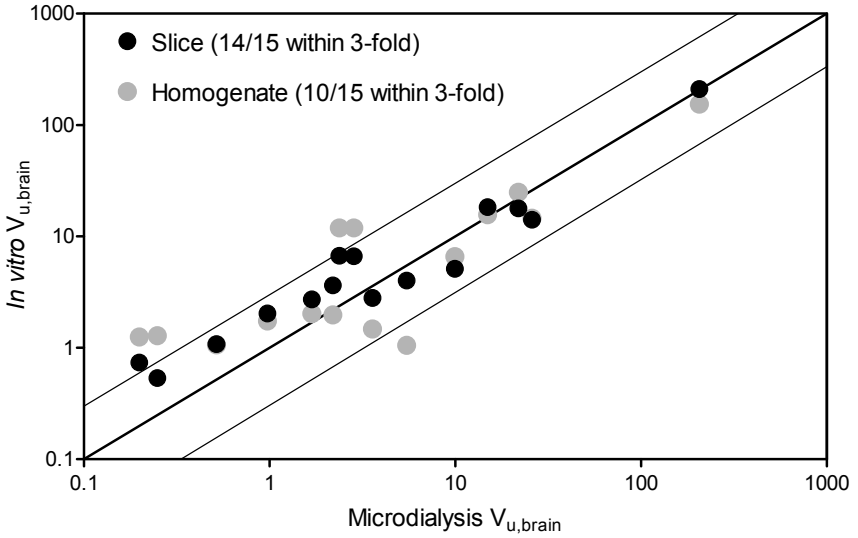

Figure 6. Relationship between $V_{u,brain}$ determined *in vivo* using microdialysis and *in vitro* using the brain homogenate method (grey filled circles) and the slice method (black filled circles).

By taking the microdialysis data as accurate, the brain slice 90% CIR of 2.95 suggests that by using the slice method only one out of ten drugs will have an estimated $V_{u,brain}$ that is more than 2.95-fold off the real value. Even though the slice method supersedes the homogenate method, a discussion is justified whether the *in vivo* agreement the slice method is satisfactory. Needless to say, it depends on the question asked. For methods used in drug discovery differences within 3-fold are commonly said to be acceptable or even indicative of equivalence between methods. However, rather than making claims that the method performance is sufficient for early drug discovery screening, the question must be asked here: what is realistically the accuracy of literature microdialysis data. That is to say what 90% CIR would hypothetically result when comparing microdialysis data generated at two independent labs? While there is no answer to this question, we know that all methods hold experimental variability (random error), and to some extent also systematic error (inaccuracies). Nevertheless, microdialysis is the only method to measure unbound drug exclusively *in vivo*, and therefore the method of choice for evaluating the slice and homogenate methods. The standpoint obtained from Paper I, is that the slice method is in overall agreement with microdialysis and that there were no major issues raised concerning the

applicability of the method. A similar conclusion was recently arrived at by Liu et al. who found a within 3-fold agreement for a majority of compounds between the homogenate method and microdialysis [79].

4.2 Unbound intracellular drug concentrations

The abovementioned discrepancies between the slice and homogenate method for basic drugs triggered the definition of a new parameter: the unbound partition coefficient of the cell ($K_{p,uu,cell}$). $K_{p,uu,cell}$ describes the intracellular exposure to unbound drug as the unbound intra-to-extracellular concentration ratio (Eq. 19) where $C_{u,cell}$ is the averaged unbound intracellular drug concentration of an "average" brain cell.

$$K_{p,uu,cell} = \frac{C_{u,cell}}{C_{u,brainISF}} \tag{19}$$

It is proposed in Paper I that $K_{p,uu,cell}$ can be experimentally determined by combining the brain slice and the homogenate methods. This is because the slice $V_{u,brain}$ describes the net uptake of drug into cells, irrespective of mechanism, whereas the homogenate method gives specific information on intracellular binding. The developed principles and methodology, which differentiates intracellular binding from other uptake processes, may be applicable also in other fields of research pertaining to cellular uptake e.g. prediction of hepatic drug clearance. It should be noted at this point, however, that there are assumptions associated which may be difficult to justify for all kinds of drugs, such as the existence of a single intracellular compartment.

4.3 Optimization of the brain slice method

As the position was taken, based on findings in Paper I, that the brain slice method has a promising application for measurement of $K_{p,uu,brain}$, a thorough investigation of the experimental setup was warranted. Various aspects of the experimental setup and properties of the slices were addressed and resulted in the final (optimized) protocol described in Section 3.4.2.

The most urgent issue to be resolved was the applicability of the slice method to highly lipophilic drugs with high $V_{u,brain}$. Data for lipophilic basic compound using the preliminary setup had indicated that equilibrium may not be reached within the four hours incubation used. Taking thioridazine as example (Fig. 7) it was shown that the time to reach equilibrium was dramatically reduced by improving the stirring efficiency by using slow rotational shaking in a relatively large incubation vessel. The equilibrium was further

accelerated to be reached within 5 hours incubation by increasing the amount of tissue per unit of buffer volume by adding all six slices into the same incubation vessel. Since thioridazine and rimonabant represent the extremes of drug lipophilicity it was concluded that 5 hours incubation would be an appropriate default incubation time.

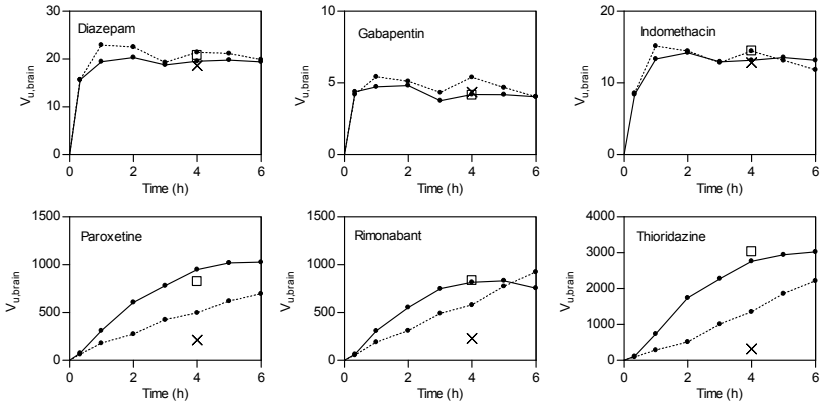

Figure 7. Brain slice uptake experiments with a cassette of six model compounds. Samples were taken at 0.33, 1, 2, 3, 4, 5 and 6 hours. The solid and fine lines represent incubations with 6 slices and 1 slice per incubation dish, respectively. Open squares represent the $V_{u,brain}$ in incubations with single compounds. The cross represents the $V_{u,brain}$ as determined using the protocol in Paper I.

Simplifications were made to the protocol in order to increase throughput and minimize the amount of work associated with the generation of data for new compounds. The amendment with the greatest leverage for throughput was the introduction of cassette incubations. There were no indications of significant differences between $V_{u,brain}$ determined in incubations of single compounds as compared to cassette incubations (Fig. 7). To obtain an indication of the appropriate upper limit for the number of drugs to be pooled, the concentration dependence of a single compound (paroxetine) was studied. The results showed that $V_{u,brain}$ was constant up to a buffer concentration of 1 µM above which $V_{u,brain}$ was dramatically reduced. Based on this experiment as well as on analytical considerations it was considered prudent to limit the number of drugs to 10 and to use a collective drug concentration in buffer not exceeding 1 µM.

Finally, the various sources of variability were investigated. The variability associated with performing the experiment in different slices amounted to 45% of total variability, whereas analytical variability contributed with 35%. The smaller remaining variability was related to using different rats and performing the experiment on different days. Simulated standard error resulting from various design scenarios indicated that determination of $V_{u,brain}$ in six

slices from a single rat on a single day was the best trade-off between work input and precision of $V_{u,brain}$.

4.4 Development of a correction model for drug in residual blood

On the course of generating the dataset of $K_{p,uu,brain}$ to be used in Paper IV, it was observed for a large number of drugs that the estimated value for A_{brain} was very variable between animals and sometimes negative after having made the correction for the amount of drug in residual blood. It was evident that the correction model initially used based on 3 % residual blood was inappropriate. If those compounds would have been simply excluded from the study, it would have biased the dataset and limited the applicability domain of the prediction model for $K_{p,uu,brain}$. Alternatively, assignment of very low values for $K_{p,brain}$ could be justified since low $K_{p,brain}$ is the root of the problem. However, the same cannot be done for the corresponding value for $K_{p,uu,brain}$ since low $K_{p,brain}$ can arise not only from $K_{p,uu,brain}$ being low but also from the extent of plasma protein binding greatly exceeding binding in brain tissue i.e. when the product of $f_{u,p}$ and $V_{u,brain}$ is small (Eq. 6). It was therefore necessary to revise the correction model for residual blood.

The improvement of accurate and precise correction for drug in residual blood was done in five sequential steps: First, the procedures for exsanguination of the animal and sampling of tissue were standardized so as to minimize the amount of residual blood. This was assessed by visual inspection.

Second, while using these exact procedures (Section 3.5) the volumes occupied by residual plasma water (V_{water}), plasma proteins ($V_{protein}$) and erythrocytes (V_{er}) were experimentally determined in a group of 8 rats. The intention was to determine these values "once and for all" so as to be generally applicable for residual blood correction. V_{water} (10.3 ± 0.54 µl/g_brain) was slightly higher than $V_{protein}$ indicating that the concentration of plasma proteins is lower in brain residual plasma than in arterial plasma. Similarly the V_{er} (2.13 ± 0.68 µl/g_brain) was very low compared to V_{water} which indicated a lower hematocrit of brain residual blood.

In the third step, a drug-specific correction model was constructed that accommodates the binding of drug to plasma proteins and erythrocytes. This resulted in Eq. 20, which expresses $K_{p,uu,brain}$ as a function of totally nine measured variables including the abovementioned variables as well as the drug concentration in whole blood (C_{blood}) and arterial hematocrit (Hct).

$$K_{p,uu,brain} = \frac{C_{brain,h} - \left[\left(V_{water} \times C_p \times f_{u,p} \right) + \left(V_{er} \times \frac{C_{blood} - (1 - Hct) \times C_p}{Hct} \right) + \left(V_{protein} \times C_p \times (1 - f_{u,p}) \right) \right]}{(1 - V_{water} - V_{er}) \times V_{u,brain} \times C_p \times f_u} \quad (20)$$

In the fourth step, the correction model was applied to the measurement of $K_{p,uu,brain}$ for moxalactam, indomethacin and loperamide out which the first two had negative values of $K_{p,uu,brain}$ using the previous correction method. Overall, the results showed a significant added value since all estimates of $K_{p,uu,brain}$ were non-negative, and the precision of $K_{p,uu,brain}$ were within an acceptable range given the circumstances (Fig. 8).

The final step towards accurate, precise and yet practical correction approach was to identify and make the appropriate simplifications. First it was deduced that the amount of drug associated with erythrocytes could be generally ignored. Hence, measurements of C_{blood} and Hct were avoided. Secondly, statistical analysis of the contribution to imprecision of $K_{p,uu,brain}$ imposed by the different measured variables, suggested that there is little benefit of measuring V_{water} and $V_{protein}$ in each animal instead of using the average values. As result, a simplified correction model was proposed (Eqs. 13-14, Section 1.3.2.4) that does not require any additional measurements. It should be noted, however, that in order to apply average values of V_{water} and $V_{protein}$, similar procedures should be used for the sampling of brain tissue.

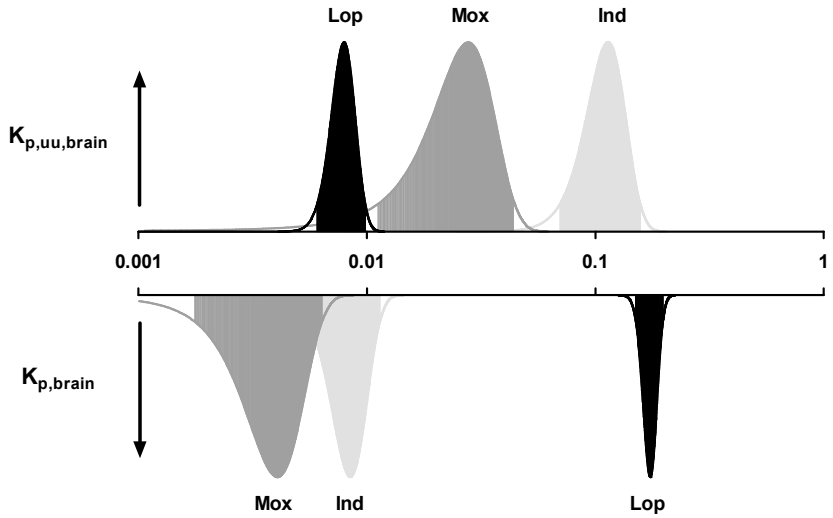

Figure 8. Probability density graph for $K_{p,uu,brain}$ (upward) and $K_{p,brain}$ (downward) for indomethacin (Ind), loperamide (Lop) and moxalactam (Mox) in a representative rat. The shaded areas define the 95 % confidence intervals. The shift on the log scale for the peak of $K_{p,brain}$ and $K_{p,uu,brain}$ corresponds to the pattern of binding to plasma proteins and brain tissue ($f_{u,p} \times V_{u,brain}$) for each drug.

A rather illuminating aspect of the work presented in Paper III was the comparison of the unbound ($K_{p,uu,brain}$) and total ($K_{p,brain}$) brain-to-plasma ratios as was done in Fig. 8. The three drugs provide a most compelling case of how one must not be mislead to make interpretations of $K_{p,brain}$ in terms of brain exposure, not even as a first approximation. This is because the rank order of the drugs can be completely reversed: loperamide being a good Pgp-substrate [80] has the lowest $K_{p,uu,brain}$, but owing to its large $f_{u,p} \times V_{u,brain}$ product it has the highest value for $K_{p,brain}$. In contrast, indomethacin and moxalactam with much smaller $f_{u,p} \times V_{u,brain}$ products had very low (previously undetectable) $K_{p,brain}$ but much higher $K_{p,uu,brain}$ than that of loperamide.

Furthermore, it is commonly assumed that total drug concentrations in the brain (logBB or $K_{p,brain}$) can be used to provide at least some indication as to "whether or not" a drug crosses the BBB. The inaccuracy of this assumption is clearly demonstrated by the indomethacin example discussed above; even when $K_{p,brain}$ is low, it is essential to estimate $f_{u,p}$ and $V_{u,brain}$ to obtain even the faintest idea of drug exposure in the brain.

4.5 Structure - brain exposure relationships

By using the very same experimental methods that were developed in Papers I-III a reasonably large dataset of $K_{p,uu,brain}$ and $K_{p,uu,CSF}$ was obtained (Table 1). The intention of generating this data set was to explore the relationship between the chemical structure of the drug and the level of unbound drug exposure in the brain. Owing to the lack of efficient methods to measure $K_{p,uu,brain}$, previously published computational prediction models have been derived from measurements of $K_{p,brain}$ (logBB) or measures of rate of BBB transport (CL_{in}).

$K_{p,uu,brain}$ was successfully determined *in vivo* for 41 of the 43 studied compounds. Overall, the findings showed that active efflux dominates drug disposition in the brain, since 34 of 41 drugs had $K_{p,uu,brain}$ values less than unity and only 7 drugs having values slightly greater than unity. The range of $K_{p,uu,brain}$ was from 0.006 for methotrexate to 2.0 for buproprion, i.e. 300-fold. In contrast, $K_{p,brain}$ ranged from ~ 0.002 for sulphasalazine to 20 for amitriptyline, i.e. 10 000-fold. This is a considerably larger range than that for $K_{p,uu,brain}$.

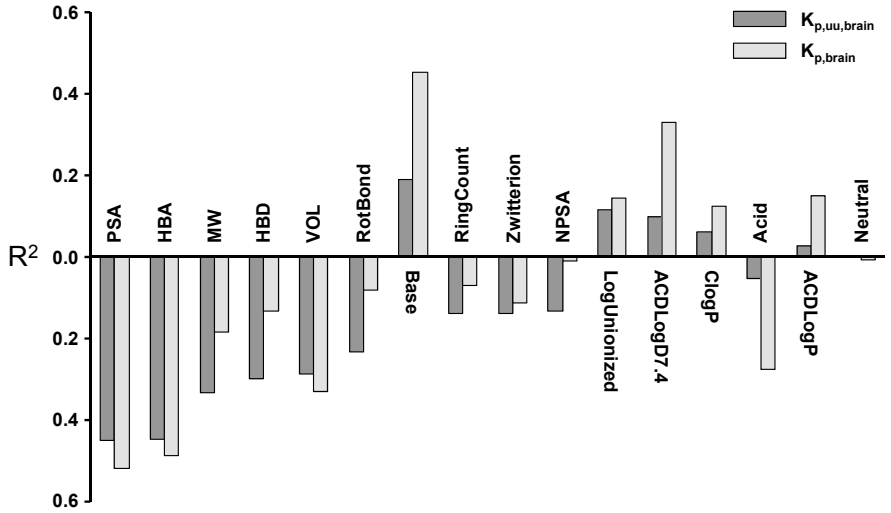

Figure 9. Linear correlation coefficient, R^2, for $K_{p,uu,brain}$, $K_{p,brain}$ and each of the 16 molecular descriptors for the selected drugs in the training data set. The upward and downward orientation of the bars represents positive and negative correlations, respectively, with $K_{p,uu,brain}$ and $K_{p,brain}$.

4.5.1 *In silico* models for $K_{p,uu,brain}$

The most significant molecular descriptors for the relationship with $K_{p,uu,brain}$ were those that relate to hydrogen bonding, i.e. PSA and HBA (Fig. 9). The first PLS model of $K_{p,uu,brain}$ used all 16 molecular descriptors simultaneously as variables and was also the model with the best predictivity (Q^2=0.452). However, a large number of variables did not significantly contribute to the model and were excluded in a step-wise manner. The simplest models contained only descriptors of hydrogen bonding (PSA, HBA) and were equally predictive. The very simplest model (Eq. 21, Fig. 10) used HBA as the single descriptor (Q^2 = 0.426, RMSE = 3.94-fold):

$$\log K_{p,uu,brain} = -0.04 - 0.14 \times HBA \qquad (21)$$

The dataset was not large enough to be divided into a training-set and a test set of compounds. Therefore an external validation dataset was established from collated literature data using the brain homogenate method. The data in the external dataset appeared to be equally well predicted (RMSE = 4.19-fold) with very little bias (Fig. 10).

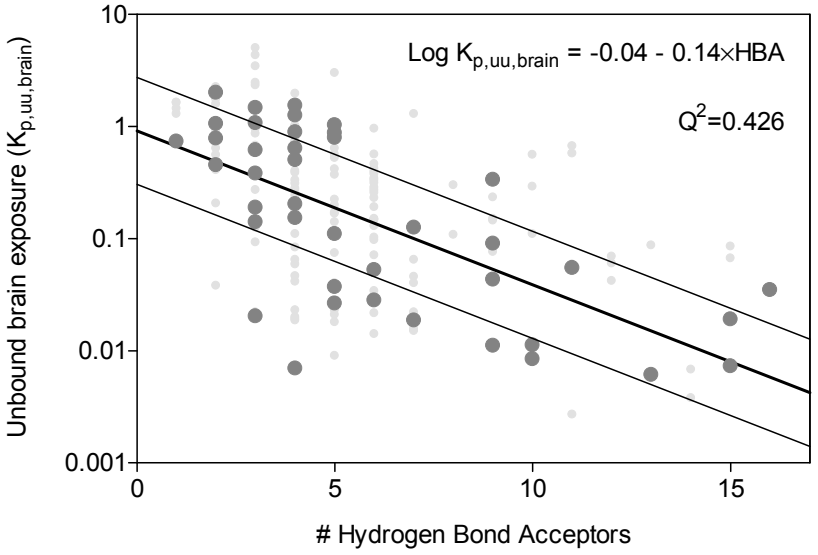

Figure 10. Observed versus predicted rat $K_{p,uu,brain}$ based on Eq. 21. Large grey filled circles are drugs in the training-set. Small grey filled circles are observations from the external dataset. Solid lines represent the prediction model and fine lines represent a 3-fold error of prediction.

The model can be readily interpreted in terms of the expected pharmacology of the drug; in order to achieve a 2-fold increase in $K_{p,uu,brain}$, it is necessary to remove 2 HBAs from the molecular structure. Conversely, a 2-fold reduction in $K_{p,uu,brain}$ can be achieved by addition of 2 HBAs. A change in $K_{p,uu,brain}$ as small as 2-fold can be considered pharmacologically significant since it principally means a doubling of the dose if the drug acts on a central target. If, on the other hand, there are critical CNS side effects associated with a peripherally acting drug, a reduction in $K_{p,uu,brain}$ by a factor 2 results in doubling of the therapeutic window.

The Q^2 value for the model predictivity provides the proportion of the variability in $K_{p,uu,brain}$ between drugs that was explained by the model. The presented models were capable of explaining only 40-45% of the variability in the training-set. It follows, therefore, that other approaches are required than adding/removing hydrogen bond acceptors in order to fully maximize or minimize $K_{p,uu,brain}$. Strategies for improving model predictivity include the construction of local models that are specific to a particular class of drugs or to apply different computational methods that also accommodate non-linear relationships. However, the challenge of predicting the simultaneous influence of all known and unknown transporters at the BBB cannot be overestimated.

A question of fundamental interest is the mechanistic background for the relationship between $K_{p,uu,brain}$ and hydrogen bonding; is it related to effects

on passive transport, such as for oral drug absorption [65], or is it related to both passive and active processes? An isolated effect on passive transport appears unlikely since it would imply a basal level of efflux for all drugs. Instead, a dual of role of hydrogen bonding is suggested where formation of hydrogen bonds is related to passive transport as well as being important for the interaction with transporters such as Pgp [16].

Interestingly, lipophilicity, which is normally correlated with passive transport, did not increase the value of $K_{p,uu,brain}$. It is plausible that the effect of increased passive transport by increased lipophilicity is paralleled and offset by increased efflux owing to increased drug concentrations in the membrane where the interaction takes place between drug and transporter (Pgp). Hence, the dominating position of hydrogen bonding for structure-brain exposure relationships seems to arise from its additive effects on passive and active transport independently of lipophilicity; a less lipophilic drug with many HBAs has very limited passive transport and is thus sensitive to low capacity active efflux, while a lipophilic drug with many HBAs is a probable transporter substrate, e.g. a Pgp substrate [81].

4.5.2 *In silico* models for $K_{p,brain}$ (logBB)

Since logBB has previously been the most commonly used experimental measure in computational prediction models, models for $K_{p,brain}$ or logBB, were also investigated in Paper IV.

The relationship between logBB and structure was dominated by hydrogen bonding similar to $K_{p,uu,brain}$. In contrast to $K_{p,uu,brain}$, however, logBB was also positively correlated with descriptors of lipophilicity. Furthermore, logBB is higher for basic drugs than for acidic drugs (Fig. 9). The PLS model that was developed contained one descriptor for hydrogen bonding (HBA), one descriptor of lipophilicity (ACDLogD7.4) and the ion class of the drug (acid or base):

$$\log BB = -0.18 - 0.097\,HBA + 0.10\,ACD\log D7.4 + 0.68\,Base - 0.67\,Acid \quad (22)$$

The predictivity of the logBB model was better than the $K_{p,uu,brain}$ model based on comparison of Q^2 (0.693 vs. 0.426). The better Q^2 value of the logBB model should be seen in the light of the 30-fold greater range of observed values. In contrast, similar predictivity is seen based on RMSE (4.0-fold vs. 3.9-fold). While interpreting the relationships between molecular descriptors and logBB it should be born in mind that logBB is a hybrid parameter containing information on both brain exposure ($K_{p,uu,brain}$) and the pattern of brain tissue vs. plasma protein binding i.e. the $V_{u,brain} \times f_{u,p}$ product:

$$BB = K_{p,uu,brain} \times V_{u,brain} \times f_{u,p} \quad (23)$$

Hence there is a straightforward interpretation of the logBB model: HBA accounts for the part of logBB which is, in fact, related to $K_{p,uu,brain}$; AC-DLogD7.4 and the drug being basic accounts for binding to phospholipid in tissue ($V_{u,brain}$); and the drug being acidic accounts for extensive binding to albumin in plasma ($f_{u,p}$). The imminent risk of relying on logBB-derived prediction models is the design of drugs that are unnecessarily lipophilic or basic without improved unbound brain exposure; or if restricted brain exposure is desired, the design of albumin bound acidic compounds that later prove to have significant CNS effects at therapeutic plasma concentrations.

4.6 Utility of $K_{p,uu,CSF}$ as a surrogate for $K_{p,uu,brain}$ in the rat

The data collected in Paper IV (Table 1) allowed a direct comparison of $K_{p,uu,CSF}$ and $K_{p,uu,brain}$ in the rat. The relationship shown in Fig. 11A reveals a remarkable agreement considering the physiological differences; $K_{p,uu,CSF}$ was within 3-fold of $K_{p,uu,brain}$ for 32 of 39 drugs (r^2=0.80). The slope of the regression line (0.71) was significantly different from 1 ($p < 0.0001$), which indicated that there were systematic, however moderate, differences between $K_{p,uu,CSF}$ and $K_{p,uu,brain}$. In particular, low values for $K_{p,uu,brain}$ were associated with proportionally higher values for $K_{p,uu,CSF}$. All four drugs for which $K_{p,uu,CSF}$ was more than 3-fold greater than $K_{p,uu,brain}$ were Pgp substrates: loperamide, nelfinavir, rifampicin and verapamil. The explanation is most likely found in the differential expression and role of Pgp in the BBB vs. BCSFB. While Pgp is the most abundant efflux transporter in the rat BBB, its role at the BSCFB is unclear since the apical or sub-apical localization infers net drug influx in the blood-to-CSF direction [82, 83]. While these results strongly indicate a risk of over predicting $K_{p,uu,brain}$ for Pgp substrates, further studies are needed to establish if it can be generalized to all Pgp substrates.

The under-prediction of $K_{p,uu,brain}$ for drugs with higher values (Fig. 11A) is more intriguing. It can be principally explained by less efficient active drug influx at the BCSFB as compared to the BBB, which is conceivably due to the lack of specific transporters at the BCSFB. If this was the case, one might have expected values for $K_{p,uu,brain}$ to be greater than unity. However, active influx and efflux work simultaneously in opposite directions to produce principally any value for $K_{p,uu,brain}$. The group of drugs for which $K_{p,uu,CSF}$ under-predicted $K_{p,uu,brain}$ mainly comprised moderately lipophilic basic drugs. The identity of the supposed uptake transporters is unclear however may relate to a new “pyrilamine transporter”, which is an energy-

dependent, proton-coupled anti-porter interacting with organic cations. Oxycodone and diphenhydramine for which $K_{p,uu,brain}$ was underpredicted by $K_{p,uu,CSF}$ in this study are reported to be substrates of this transporter [84, 85].

Overall, the relatively strong relationship between rat $K_{p,uu,CSF}$ and $K_{p,uu,brain}$ supports the use of $K_{p,uu,CSF}$ for cross-species comparison of brain exposure data (Section 4.7). The relationship is however not sufficiently strong to justify replacement of the experimental determination of $K_{p,uu,brain}$ in small rodents. This is especially so since measurements of $K_{p,uu,brain}$ and $K_{p,uu,CSF}$ are of comparable experimental complexity when using the methodologies developed in Papers I-III.

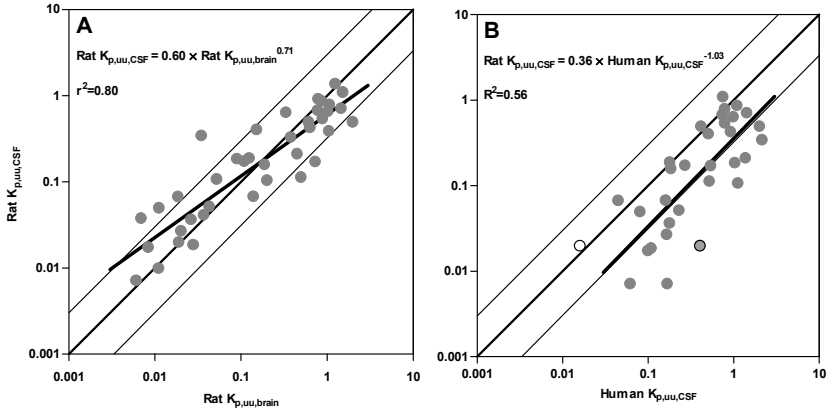

Figure 11. Relationship between $K_{p,uu,CSF}$ and $K_{p,uu,brain}$ in the rat (A) and the agreement between rat and human $K_{p,uu,CSF}$ (B). Fine lines represent identity and 3-fold differences. Solid lines are the result of linear regression analysis of log-transformed data. Data points represent average values for one drug. Moxalactam (circles) was included from both a study in patients with bacterial meningitis (filled circle) and a study in healthy volunteers (open circle) (B).

Table 1. *Brain exposure ratios in the rat and humans*

		Rat data						Human data
	HBA	$C_{u,p}$ (μM)	$V_{u,brain}$ (mL/g_brain)	$f_{u,p}$	$K_{p,brain}$	$K_{p,uu,brain}$	$K_{p,uu,CSF}$	$K_{p,uu,CSF}$
Alprenolol	3	0.28	50	0.44	8.27	0.38	0.33	-
Amitriptyline	1	0.022	310	0.09	20.15	0.73	0.17	0.18
Atenolol	5	1.5	2.5	1.0	0.07	0.026	0.036	0.54
Baclofen	3	4.2	1.7	1.0	0.03	0.020	0.027	0.17
Bupropion	2	0.079	16	0.31	9.78	2.00	0.49	2.0
Cefotaxime	12	2.8	[a]	0.59	[a]	[a]	0.007	0.17
Codeine	4	0.21	3.2	0.95	2.70	0.89	0.54	0.79
Delavirdine	9	0.017	40	0.016	0.03	0.043	0.051	0.23
Diazepam	3	0.061	20	0.12	2.28	1.07	0.78	0.79
Diphenhydramine	2	0.051	32	0.48	16.25	1.05	0.39	-
Ethyl-phenylmalonamide	4	4.3	0.9	0.55	0.64	1.25	1.4	-
Gabapentin	3	5.2	4.6	1.0	0.64	0.14	0.067	0.16
Indomethacin	5	0.20	14	0.01	0.01	0.11	0.17	0.27
Lamotrigine	5	1.8	4.6	0.51	2.02	0.88	0.86	1.10
Levofloxacin	7	0.59	1.7	0.82	0.17	0.12	0.19	0.18
Loperamide	4	0.054	370	0.06	0.15	0.007	0.037	-
M3G	10	2.7	0.60	1.00	0.007	0.011	0.049	0.081
M6G	10	2.1	0.99	0.98	0.008	0.008	0.017	0.10
Methotrexate	13	2.9	0.68	1.00	0.004	0.006	0.007	0.062
Metoprolol	4	0.75	5.5	0.90	3.14	0.64	0.43	0.93
Morphine	4	0.23	3.7	0.90	0.51	0.15	0.40	0.51
Moxalactam	15	3.8	0.57	0.32	0.003	0.019	0.020	0.41
Nadolol	5	0.78	3.4	0.86	0.11	0.037	0.041	-
Nelfinavir	7	0.0019	860	0.00	0.04	0.019	0.067	0.045
Nitrofurantoin	9	0.71	1.6	0.48	0.008	0.011	0.0099	-
Norfloxacin	6	0.70	2.9	0.87	0.07	0.028	0.018	0.11
Oxprenolol	4	0.21	11.8	0.45	1.06	0.20	0.10	-
Oxycodone	5	0.33	4.2	0.87	3.77	1.03	0.65	-
Oxymorphone	5	0.24	4.0	0.73	2.29	0.79	0.91	-
Paclitaxel	15	0.016	769	0.05	0.28	0.007	[b]	-
Pindolol	4	0.16	7.2	0.43	1.56	0.50	0.11	0.52
Propranolol	3	0.051	118	0.09	6.59	0.61	0.49	0.42
Rifampicin	16	0.83	6.9	0.12	0.03	0.035	0.34	2.2
Salicylic acid	3	5.6	1.0	0.28	0.05	0.19	0.16	0.19
Saquinavir	11	0.0030	208	0.007	0.08	0.055	[b]	0.096
Sulphasalazine	9	0.013	4.2	0.005	0.002[c]	[c]	0.032	-
Tacrine	2	0.12	22	0.55	9.56	0.78	0.67	0.74
Thiopental	4	0.55	4.3	0.19	1.28	1.53	1.09	0.75
Thioridazine	2	0.0013	3333	0.002	3.75	0.45	0.21	1.4
Topiramate	9	3.4	3.2	0.79	0.84	0.33	0.63	1.00
Tramadol	3	0.30	4.2	0.85	5.29	1.46	0.71	1.44
Verapamil	6	0.075	54	0.12	0.34	0.053	0.11	1.13
Zidovudine	9	1.2	1.1	0.64	0.065	0.090	0.18	1.04

[a] Instability in brain homogenate

[b] Below limit of quantification

[c] Unacceptably large variability in $K_{p,brain}$ and $K_{p,uu,brain}$ due to the correction made for drug in vascular spaces.

4.7 Agreement between $K_{p,uu,CSF}$ in rat and humans

The relevance to humans of structure-brain exposure relationships in the rat (Section 4.5) was evaluated by comparing $K_{p,uu,CSF}$ determined in rats and human patients. The relationship between rat and human $K_{p,uu,CSF}$ (r^2=0.55, Fig. 11B) is considered reasonably strong given the magnitude of normal experimental variability and the diversity of collected human data. There was, however, a bias toward the observed human $K_{p,uu,CSF}$ values being on average 3-fold higher than the corresponding values in the rat.

By taking the human and rat data as accurate, the bias is interpreted as the rat having developed CNS barriers which are capable of providing a higher level of protection from exogenous compounds than humans. This could involve several aspects of the CNS barriers such as the physical tightness, the efficiency and expression of various transporters or the fluid dynamics of the brain.

While the biological explanations mentioned above are plausible, the bias may also have resulted from the combined effect of experimental factors that incidentally are expected to contribute to a bias in the observed direction. These methodological issues were: 1) the disease state of the patients, 2) kinetic bias due to timing of CSF sampling and 3) the different CSF sources used for rat (cisternal) and human (lumbar). Firstly, and most importantly, the subjects of the clinical reports were typically not healthy volunteers but patients with various disease states several of which are associated with alterations in CNS barrier function and sometimes increased protein contents in the CSF. This is exemplified by moxalactam for which the $K_{p,uu,CSF}$ was 25-fold lower in healthy volunteers than in patients with bacterial meningitis (Fig. 11B).

The second experimental reason for the observed rat/human $K_{p,uu,CSF}$ difference may be a delay in appearance and elimination of drug in the CSF relative to plasma, which makes the dosage regimen and the timing of CSF sampling critical. Ideally, the CSF and plasma would be sampled simultaneously at steady state during continuous intravenous infusion. This was rarely performed in humans and, since the single CSF sample was generally taken several hours after the last dose, it is almost certain that a kinetic bias was introduced towards higher values of $K_{p,uu,CSF}$ in humans. This is contrasted by the rat experiments, where 4-hour intravenous infusions were given to rats to approach steady state and where $K_{p,uu,CSF}$ would be underestimated for any drug for which 4 hours was not sufficient to attain complete equilibrium.

Thirdly, $K_{p,uu,CSF}$ was determined using CSF samples from *cisterna magna* in the rat and generally by lumbar puncture in the patients. The impact of different sampling sites on the $K_{p,uu,CSF}$ comparison will depend on the extent of drug exchange between the CSF and the blood via the blood-spinal cord barrier and cord tissue along the path of CSF flow. Although the blood-

spinal cord barrier is similar to the BBB in terms of cellular structure, it is generally more permeable than the BBB [86]. Therefore, the value of $K_{p,uu,CSF}$ is expected to be higher from lumbar samples if there is significant drug exchange with blood across the blood-spinal cord barrier. If, on the other hand, drug exchange is not significant, lumbar CSF would reflect cranial CSF with a lag time of 60-90 minutes [87] thus potentiating the kinetic bias discussed above. Either way, given the general timing of CSF sampling in the clinical material, human $K_{p,uu,CSF}$ from the lumbar sampling site is expected to be overestimated to some extent relative to the rat.

It cannot be concluded from the present data whether the 3-fold difference reflects a true species difference, an observational bias, or both. Nevertheless, the similar rank-order (correlation) for the drugs justifies the established practice in drug industry to use rats for the study of central drug exposure and to derive *in silico* prediction models.

5 Conclusions and perspectives

This thesis was directed towards developing a simple and efficient methodology for measuring the unbound drug concentration in brain tissue in experimental animals. The developed methodology was based on the idea that the unbound drug concentration can be assessed by combining conventional *in vivo* measurements of the total (bound plus unbound) brain tissue concentration with a separate *in vitro* determination of the degree of drug binding in the brain. The first study (Paper I) verified the validity of this combined *in vivo - in vitro* approach. It was shown that a brain slice method, but not a brain homogenate method, gave results that were similar to measurements using the *in vivo* microdialysis technique. Thereafter, improvements were made to the experimental setup of brain slice method making it both high-throughput and amenable to the study of drugs with diverse chemical properties including those with high lipophilicity.

The third study (Paper III) elaborated on the correction for drug in residual blood, which is a well-known problem when determining very low levels of total drug in the brain. It was concluded that by using standardized procedures and statistics it is possible to obtain measurements with defined precision also for drugs that were previously considered "not detectable".

In previous years, there were no methods available to determine the unbound drug concentration in tissue; the microdialysis technique, which emerged in the 1990s, was too complex to gain widespread use in drug industry. As resulting from the lack of methods to generate data, the unbound drug concentration in the brain as defining brain exposure was never fully recognized among scientists. Instead, surrogate measurements of the total drug concentration have shaped fundamental ideas pertaining to the relationship between the chemical properties of the drug and the level of exposure in the brain. For example, it is today considered common knowledge that high lipid solubility of the drug is associated with higher exposure in the brain.

The last study (Paper IV) in which a novel 43-drug dataset was presented, was the first study to show the relationship between chemical drug properties and the exposure of the brain to *unbound* drug. As would be expected from unbound brain exposure (as opposed to total) being determined by specific drug-transporter interactions, there were no strong relationships found. The analysis showed however, that the best prediction was obtained by simply counting the number of hydrogen bond acceptors in the molecule. Whereas the dependence of hydrogen bond potential is long known, the most signifi-

cant conclusion was that there was no obvious relationship with drug lipophilicity, at odds with the common understanding.

The data collected in Paper IV was also used to evaluate the utility of CSF sampling i.e. $K_{p,uu,CSF}$ as surrogate measurement of the unbound drug concentration in the brain i.e. $K_{p,uu,brain}$. The overall agreement between $K_{p,uu,CSF}$ and $K_{p,uu,brain}$ showed that CSF can be principally used as a surrogate when there is no possibility measure $K_{p,uu,brain}$. A finding of particular interest was that drugs that are substrates for Pgp are likely to have higher concentrations in CSF than in the brain.

After having established that $K_{p,uu,CSF}$ was a reasonable surrogate for $K_{p,uu,brain}$ in the rat, the agreement between $K_{p,uu,CSF}$ in rat and human was investigated. Rat $K_{p,uu,CSF}$ was on average 3-fold lower than human $K_{p,uu,CSF}$, but it cannot be concluded if this bias was due to a CNS barrier species-difference or due to artifacts in the clinical data. The main conclusion was that the overall correlation (r^2=0.56) suggests that the structure-unbound brain exposure relationships that were derived from the rat can be used for designing drugs for man.

The methods developed in this thesis are valuable tools in drug discovery to study the effect of the blood-brain barrier on the incidence of central effects and side-effects for any class of drugs. Since the methods are predictive for brain exposure in humans, they can also be used to select the most appropriate compounds for further development.

Future progress in the field of predictions is likely to rely also on information from various *in vitro* methods using human material. However there are still significant challenges associated with developing approaches for scaling of *in vitro* data to the *in vivo* situation, not to mention difficulties of obtaining a critical mass of solid human data to validate such attempts.

6 Populärvetenskaplig sammanfattning

Blod-hjärnbarriären
Blodkärlen i hjärnan har en särskild beskaffenhet som skiljer sig från övriga organ; kapillärväggarna är förhållandevis svårgenomträngliga eftersom det saknas egentliga hål genom vilka näringsämnen normalt sett rör sig obehindrat. Istället är hjärnans kapillärer utrustade med s.k. bärarproteiner som ser till att koncentrationen i hjärnan av de ämnen som är nödvändiga för dess funktion hålls på en lagom nivå. Vissa varianter av dessa bärarproteiner utsöndrar samtidigt slaggprodukter som annars skulle ansamlas. Tätheten i hjärnans kapillärer har gett upphov till benämningen blod-hjärnbarriären. Denna barriär är även känd för att ge ett skydd mot kroppsfrämmande och potentiellt farliga ämnen såsom läkemedel. Skyddet som upprätthålls är alltid den kombinerade effekten av att kapillärens fysiska täthet bromsar inträdet av det främmande ämnet och att speciella bärarproteiner fortlöpande fångar upp och utsöndrar många av de molekyler som ändå tar sig in.

Betydelsen för läkemedlets effekter och framtagandet av nya läkemedel
Av uppenbara skäl kan blod-hjärnbarriären medföra problem vid utveckling av nya läkemedel som är tänkta att ha sin verkan i hjärnan. Samtidigt kan det finnas fördelar för läkemedel som ska verka i andra organ än hjärnan; om blod-hjärnbarriären effektivt hindrar läkemedlet att komma in kan detta förhindra biverkningar som annars kunnat uppstå. Ett konkret exempel på detta är den morfinliknande läkemedelssubstansen loperamid som, mer känd under produktnamnet Imodium, används för att motverka diarré. Förhållandet kan förklaras som följer; morfin som bevisligen tillåts komma in i hjärnan har dels en smärtstillande verkan i hjärnan och dels en förstoppande biverkan i tarmen. Loperamid å andra sidan hålls tack vare ett särskilt bärarprotein i blod-hjärnbarriären effektivt utanför hjärnan, varför effekter på hjärnan saknas och loperamid kan säljas receptfritt på apoteket. Den nyare typen av allergimedicin såsom ceterizin (Zyrlex) är ett liknande exempel som jämfört med äldre allergiläkemedel har betydligt lindrigare sövande effekt.

Vare sig man utvecklar läkemedel som ska verka i hjärnan eller annat organ behöver man ibland mäta koncentrationen av läkemedlet i hjärna hos ett försöksdjur t.ex. råtta. Detta görs för att säkerställa att läkemedlet verkligen når sitt effektställe, eller som i andra fall då man vill förvissa sig om att läkemedlet inte kan orsaka biverkningar där. Mätning av läkemedelskoncentration i hjärna används också för utredande studier, t.ex. om man vill ta reda

på om en ny klass av läkemedel utövar sin farmakologiska effekt i hjärnan eller någon annanstans.

Att mäta läkemedelskoncentrationen i prover av hjärnvävnad från ett avlivat försöksdjur är förhållandevis trivialt med den avancerade analysutrustning som finns att tillgå. Sådana mätningar har gjorts i läkemedelsindustrin mer eller mindre rutinmässigt under årtionden. Det stora problemet som varit otillräckligt uppmärksammat är att den uppmätta totala läkemedelskoncentrationen inte ger ett rättvisande mått på hur mycket hjärnan exponeras dvs. utsätts för läkemedlet. Detta har sin grund i att läkemedelsmolekylerna i hjärnan befinner sig i två olika former: antingen som fritt rörliga i vävnadens vatten där de är också är farmakologiskt aktiva, eller som farmakologiskt inaktiva när de är bundna i hjärnans fett. Förhållandet mellan andelen aktivt och inaktivt läkemedel har mycket att göra med läkemedlets kemiska egenskaper såsom fettlöslighet, men om detta säger den uppmätta totala koncentrationen ingenting. Om totalkoncentrationen av flera olika läkemedelssubstanser mäts och utvärderas finns det därmed begränsade chanser att välja ut den bästa. Likaledes om en lovande läkemedelssubstans ska förbättras i detta avseende genom förändring av dess kemiska struktur är det också lätt att bli vilseledd; om läkemedlet görs mer fettlösligt ökar visserligen den totala koncentrationen i hjärnan men den fria farmakologiskt aktiva koncentrationen förblir okänd. Detta anses idag ha varit ett avgörande skäl till att så många utvecklingsprojekt i läkemedelsindustrin har misslyckas.

Doktorsavhandlingen

Arbetet i denna doktorsavhandling handlar om utvecklandet av nya lättanvända metoder för att mäta den fria och aktiva läkemedelskoncentrationen i hjärnan. Principen bygger på att de traditionella mätningarna av totalkoncentration kombineras med separata provrörsförsök som för varje läkemedel bestämmer förhållandet mellan antalet fria och bundna läkemedelsmolekyler. Därvid kan den fria koncentrationen också beräknas. I delstudie 1 visades att denna princip var gångbar. I provrör med tunna snitt av råtthjärna uppmättes bindningsgraden av 15 olika läkemedel. Resultatet stämde väl överens med mätningar gjorda med den etablerade men svårbemästrade mikrodialysmetoden. Med dessa lovande resultat startades delstudie 2 för att ytterligare förbättra och förenkla hjärnsnittsmetoden för att möjliggöra snabbare testning av stora antal substanser. Delstudie 3 syftade till att göra en viktig förbättring av de traditionella mätningarna av totalkoncentrationen vilka hjärnsnittsmetoden kombineras med. I prover av hjärnvävnad finns ofrånkomligen också en viss mängd blod som också innehåller det studerade läkemedlet. Eftersom läkemedel i blod inte befinner sig i hjärnan i egentlig mening kan detta störa analysen allvarligt, och då särskilt för läkemedel med låg totalkoncentration sett i förhållande till totalkoncentrationen i blod. Den korrigering som normalt sett görs för detta visade sig under avhandlingsarbetets gång inte fungera tillfredställande, vilket föranledde ett invecklat utveck-

lingsarbete på denna punkt. Detta arbete gjorde det möjligt att erhålla noggranna mått på totalkoncentration i hjärna även för läkemedel med synnerligen låg koncentration i hjärna i förhållande till blod. Därutöver blev det möjligt att tillbakavisa en felaktig men vanlig och till synes logisk föreställning: att det traditionella användandet av totalkoncentration (utan kombinering med hjärnsnittsmetoden) kan användas för att visa om ett läkemedel inte finns i hjärnan överhuvudtaget.

I den sista delstudien, delstudie 4, användes de metoder som utvecklats i delstudier 1-3 för att skapa en unik samling av uppmätta fria läkemedelskoncentrationer i hjärna och ryggmärgsvätska för 43 läkemedel. De olika kemiska egenskaperna för de 43 läkemedlen beskrevs med siffervärden varefter ett datorprogram användes för att hitta samband mellan dessa och läkmedlens fria koncentration i hjärna. Ett sådant samband skulle kunna vägleda läkemedelskemisten när nya läkemedel ska designas och byggas ihop. Ett måttligt starkt samband hittades med de siffervärden som beskrev läkemedlets förmåga att bilda bindningar med väte, s.k. vätebindningar. Detta bekräftade tidigare slutsatser från mätningar av totalkoncentration. Mer intressant var då att det inte fanns något samband mellan läkemedlets fettlöslighet och fri läkemedelskoncentration – ett fynd som går stick i stäv med en allmänt utbredd uppfattning inom läkemedelsindustrin såväl som bland kliniker. Således för att öka den fria koncentrationen av ett läkemedel i hjärnan bör kemisten helt bortse från dess fettlöslighet och istället förändra läkemedlets struktur så att den vätebindande förmågan minskar.

I delstudie 4 gjordes även ett försök att utvärdera med vilken säkerhet man kan förutsäga hur läkemedlet hanteras av blod-hjärnbarriären i människa utifrån mätningar gjorda på råtta. Koncentrationen av de 43 läkemedlen i ryggmärgsvätska hos råtta visade sig stämma ganska väl överens med fri koncentration i hjärna i samma djur. Därmed ansågs det också relevant att för samma läkemedel jämföra koncentrationen i ryggmärgsvätska hos råtta med motsvarande mätningar som tidigare gjorts på människa. På det hela taget fanns en övertygande överensstämmelse, vilket gav ett faktamässigt underlag för användandet av råtta för utvärdering av läkemedelssubstanser i detta avseende.

Avhandlingsarbetets bidrag till läkemedelsforskningen

Forskningen i avhandlingsarbetet har tillhandahållit lättanvända försöksdjursmetoder som ger en rättvisande bild av hur blod-hjärnbarriären inverkar på nya läkemedel under utveckling. Detta öppnar möjligheter att forska fram ny kunskap, vilket exemplifieras av delstudie 4 där det fastslogs att det inte som tidigare antagits finns ett samband mellan läkemedlets fettlöslighet och dess aktiva koncentration i hjärna. Sammanfattningsvis har detta avhandlingsarbete bidragit till förbättrade beslutsunderlag i läkemedelsforskningen samt till en effektivare användning av försöksdjur.

7 Acknowledgements

The work presented in this thesis was funded by AstraZeneca R&D Mölndal and carried as collaboration between the Division of Pharmacokinetics and Drug Therapy at Uppsala University and AstraZeneca R&D Mölndal. My recurring participation in international conferences and courses was made possible by travel grants from Anna-Maria Lundins Stipendiefond, the ULLA consortium, IF:s stiftelse, Apotekare C.D. Carlssons stiftelse and the International Society for the Study of Xenobiotics.

I would like to express my sincere gratitude to all who have contributed to this thesis including:

Min handledare, professor **Margareta Hammarlund-Udenaes** för all handledning under åren. Allra särskilt tänker jag på det gedigna arbetet med manuskripten. Jag är jätteglad för detta. Tack också för att du handlett på andra plan de strikt vetenskapliga. Doktorerande åt alla!

Min biträdande handledare, **Ulf Bredberg**. Tack för alla diskussioner och alla gånger du gett mina tankar en behövlig liten knuff.

Madeleine Antonsson, tack för att du antog mig som projektarbetare från första början. Tack även för alla dina förträffliga idéer.

Gunilla Jerndal för att du antog mig till din bioanalysskola.

Fredrik Bergström för allt du har lärt mig om proteinbindning. Jag har haft väldig nytta av detta igenom hela avhandlingsarbetet.

Susanne Winiwarter för din insats genom det sista arbetet och för handledningen av QSAR modelleringen.

Hugues Dolgos and **Anders Tunek** for supporting this project.

Min vän och följeslagare inom doktorerandet **Mattias Carlström** för att du alltid hållit dörren öppen till Hotell Vinden när jag haft arbete i Uppsala. Även den gången jag annonserade min vistelse på två månader med lika många dagars framförhållning.

Min närmsta doktorandkollega **Jörgen Bengtsson**, för alla skratt och roligheter som du sprider omkring dig. Jag har haft jättekul tillsammans med dig på konferenser såväl som i vardagslivets tråk och tvång. ♪ *Put on your happy face, it´s teaching* ♪

My co-authors of the paper on the slice method, **Frederic Ducrozet** and **Brian Middleton** for conducting the study and giving me one-on-one lessons in mathematics and statistics. Stort tack även till **Henrik Nordberg** för alla tips vad gäller hanteringen av lipofila substanser.

Mina medförfattare på den kommande artikeln om slice och homogenatmetoden, **Mikael Rehngren**, **Hong Wan** för att ni genomförde studien och visat mig i hur era respektive arbetsmetoder fungerar. Jag har satt stort värde på detta.

Ingela Ahlstedt, **Ingrid Påhlman**, **Bengt von Mentzer** och **Erik Lindström** för ert engagemang i analysen av data från NK-projektet. Jag lärde mig väldigt mycket på detta även om det visade sig vara svårt.

Johan Sällström för att du alltid har svarat på kortnummer 4319 på BMC när man velat prata av sig om forskning.

Paula Holländer för att du mottog mig med sådan värme när jag började som projektarbetare med mikrodialys i Mölndal. Det var betydelsefullt.

Jennie de Verdier och **Mareike Lutz** för arbetet med att sätt upp mikrodialysmetoden.

Vrinda Nandi. It was under your kind supervision in Bangalore that I experienced my first difficulties in the lab. Even so I decided to continue in the field of preclinical PK.

Jenny Pedersen, Gustav Ahlin och **Constanze Hilgendorf** för alla spännande transportördiskussioner.

Mina exjobbare: **Marie Svanström**, **Ola Bengtsson**, **Helena Ljungqvist** och **Marie Johansson**. Tack för er värdefulla insats. Doktorerandet har varit roligast de terminer ni varit med mig.

Nuvarande och tidigare **doktorander på avdelningen i Mölndal**. Tack för alla trevliga frukostar, disputationsfester, champagnebjudningar i samband med accepterade pek mm.

Alla **bioanalytiker** och **in vivo personer** på avdelningen i Mölndal. Varenda en av er har jag någon gång rådfrågat ute på labbet. Det har alltid varit lätt och roligt att jobba med er.

Professor **Sven Björkman**, för att du delat med dig av din didaktiska erfarenhet. Jag har utöver dina kinetiska kunskaper också uppskattat dig som kemist bland hermelinerna på avdelningen.

Britt Jansson och **Jessica Strömgren** för cetirizin-analyserna respektive den tidiga (05:30) introduktionen till mikrodialysen.

Martin Bergstrand för att du lät mig vinna ett och annat set i våra svettiga pingismatcher. Därutöver tackar jag för att få ha varit en av många som gynnats av din generösa hjälpsamhet.

Tidigare och nuvarande doktorander i PK/PD gruppen och **alla på kinetikavdelnigen i Uppsala**. Jag har alltid känt mig som hemma de perioder jag varit hos er och undervisat.

Moster **Anita** och morbror **Lasse** och för tiden tillsammans i Indien. Jag minns med glädje samtalen under den rosa himlen.

Mina systrar **Carolina** och **Elin** för att ni tagit så väl hand om mig genom åren.

Pappa för att du alltid, alltid, alltid med samma intresse frågat om vad jag har för mig. Och tack för hjälpen med den populärvetenskapliga sammanfattningen. Bara Margareta är lika bra som du på att granska text.

Mamma för att du alltid varit uppmuntrande och deltagande när jag dragit hem djur av olika slag eller hittat på andra tokigheter. Kan det vara en slump att vi båda arbetat med råttor? Tack även för att du låter så många människor omfattas av din omtanke.

Noel din lille spjuver. Pappa är snart färdig med sin avhandling.

Min älskade **Maria**. Du är min stora styrka. Jag blir så glad när jag tänker på att vi har mer tid tillsammans framför oss än bakom oss. Tack för att du finns hos mig.

8 References

1. Brown RP, Delp MD, Lindstedt SL, Rhomberg LR and Beliles RP. Physiological parameter values for physiologically based pharmacokinetic models. *Toxicology & Industrial Health.* **1997,** 13, 407-484.
2. Mabuchi T, Lucero J, Feng A, Koziol JA and del Zoppo GJ. Focal cerebral ischemia preferentially affects neurons distant from their neighboring microvessels. *J.Cereb.Blood Flow Metab.* **2005,** 25, 257-266.
3. Schlageter KE, Molnar P, Lapin GD and Groothuis DR. Microvessel organization and structure in experimental brain tumors: microvessel populations with distinctive structural and functional properties. *Microvasc.Res.* **1999,** 58, 312-328.
4. Zlokovic BV. Neurovascular mechanisms of Alzheimer's neurodegeneration. *Trends Neurosci.* **2005,** 28, 202-208.
5. Davson H and Segal MB. Physiology of the CSF and Blood-Brain Barrier. **1995,**
6. Abbott NJ. Evidence for bulk flow of brain interstitial fluid: significance for physiology and pathology. *Neurochem.Int.* **2004,** 45, 545-552.
7. Sykova E and Nicholson C. Diffusion in brain extracellular space. *Physiol.Rev.* **2008,** 88, 1277-1340.
8. Shen DD, Artru AA and Adkison KK. Principles and applicability of CSF sampling for the assessment of CNS drug delivery and pharmacodynamics. *Adv.Drug Deliv.Rev.* **2004,** 56, 1825-1857.
9. Begley DJ. Delivery of therapeutic agents to the central nervous system: the problems and the possibilities. *Pharmacol.Ther.* **2004,** 104, 29-45.
10. Levin VA. Relationship of octanol/water partition coefficient and molecular weight to rat brain capillary permeability. *J.Med.Chem.* **1980,** 23, 682-684.
11. Fischer H, Gottschlich R and Seelig A. Blood-brain barrier permeation: molecular parameters governing passive diffusion. *J.Membr.Biol.* **1998,** 165, 201-211.
12. Bourasset F, Cisternino S, Temsamani J and Scherrmann JM. Evidence for an active transport of morphine-6-beta-d-glucuronide but not P-glycoprotein-mediated at the blood-brain barrier. *J.Neurochem.* **2003,** 86, 1564-1567.
13. Welty DF, Schielke GP, Vartanian MG and Taylor CP. Gabapentin anticonvulsant action in rats: disequilibrium with peak drug concentra-

tions in plasma and brain microdialysate. *Epilepsy Res.* **1993,** 16, 175-181.
14. Hediger MA, Romero MF, Peng JB, Rolfs A, Takanaga H and Bruford EA. The ABCs of solute carriers: physiological, pathological and therapeutic implications of human membrane transport proteinsIntroduction. *Pflugers Arch.* **2004,** 447, 465-468.
15. Sharom FJ. Shedding light on drug transport: structure and function of the P-glycoprotein multidrug transporter (ABCB1). *Biochem.Cell Biol.* **2006,** 84, 979-992.
16. Seelig A. A general pattern for substrate recognition by P-glycoprotein. *Eur.J.Biochem.* **1998,** 251, 252-261.
17. Nicolazzo JA and Katneni K. Drug transport across the blood-brain barrier and the impact of breast cancer resistance protein (ABCG2). *Curr.Top.Med.Chem.* **2009,** 9, 130-147.
18. Enokizono J, Kusuhara H, Ose A, Schinkel AH and Sugiyama Y. Quantitative investigation of the role of breast cancer resistance protein (Bcrp/Abcg2) in limiting brain and testis penetration of xenobiotic compounds. *Drug Metab.Dispos.* **2008,** 36, 995-1002.
19. Kikuchi R, Kusuhara H, Sugiyama D and Sugiyama Y. Contribution of organic anion transporter 3 (Slc22a8) to the elimination of p-aminohippuric acid and benzylpenicillin across the blood-brain barrier. *Journal of Pharmacology & Experimental Therapeutics.* **2003,** 306, 51-58.
20. Mori S, Ohtsuki S, Takanaga H, Kikkawa T, Kang YS and Terasaki T. Organic anion transporter 3 is involved in the brain-to-blood efflux transport of thiopurine nucleobase analogs. *J.Neurochem.* **2004,** 90, 931-941.
21. Mori S, Takanaga H, Ohtsuki S, Deguchi T, Kang YS, Hosoya K*, et al*. Rat organic anion transporter 3 (rOAT3) is responsible for brain-to-blood efflux of homovanillic acid at the abluminal membrane of brain capillary endothelial cells. *Journal of Cerebral Blood Flow & Metabolism.* **2003,** 23, 432-440.
22. Bradbury MW, Cserr HF and Westrop RJ. Drainage of cerebral interstitial fluid into deep cervical lymph of the rabbit. *Am.J.Physiol.* **1981,** 240, F329-36.
23. Cserr HF, Cooper DN, Suri PK and Patlak CS. Efflux of radiolabeled polyethylene glycols and albumin from rat brain. *Am.J.Physiol.* **1981,** 240, F319-28.
24. Szentistvanyi I, Patlak CS, Ellis RA and Cserr HF. Drainage of interstitial fluid from different regions of rat brain. *Am.J.Physiol.* **1984,** 246, F835-44.
25. Groothuis DR, Vavra MW, Schlageter KE, Kang EW, Itskovich AC, Hertzler S*, et al*. Efflux of drugs and solutes from brain: the interactive roles of diffusional transcapillary transport, bulk flow and capillary transporters. *J.Cereb.Blood Flow Metab.* **2007,** 27, 43-56.

26. Dutheil F, Beaune P and Loriot MA. Xenobiotic metabolizing enzymes in the central nervous system: Contribution of cytochrome P450 enzymes in normal and pathological human brain. *Biochimie.* **2008,** 90, 426-436.
27. Miksys S, Rao Y, Sellers EM, Kwan M, Mendis D and Tyndale RF. Regional and cellular distribution of CYP2D subfamily members in rat brain. *Xenobiotica.* **2000,** 30, 547-564.
28. Freitas RJ. Cell membrane, in Nanomedicine, volume I: Basic capabilites. **1999,** Landes Bioscience, Georgetown.
29. Wang Y and Welty DF. The simultaneous estimation of the influx and efflux blood-brain barrier permeabilities of gabapentin using a microdialysis-pharmacokinetic approach. *Pharm.Res.* **1996,** 13, 398-403.
30. Takasawa K, Terasaki T, Suzuki H, Ooie T and Sugiyama Y. Distributed model analysis of 3'-azido-3'-deoxythymidine and 2',3'-dideoxyinosine distribution in brain tissue and cerebrospinal fluid. *Journal of Pharmacology & Experimental Therapeutics.* **1997,** 282, 1509-1517.
31. Gupta A, Chatelain P, Massingham R, Jonsson EN and Hammarlund-Udenaes M. Brain distribution of cetirizine enantiomers: comparison of three different tissue-to-plasma partition coefficients: K(p), K(p,u), and K(p,uu). *Drug Metabolism & Disposition.* **2006,** 34, 318-323.
32. Xie R, Bouw MR and Hammarlund-Udenaes M. Modelling of the blood-brain barrier transport of morphine-3-glucuronide studied using microdialysis in the rat: involvement of probenecid-sensitive transport. *British Journal of Pharmacology.* **2000,** 131, 1784-1792.
33. Hammarlund-Udenaes M, Friden M, S. S and Gupta A. On The Rate and Extent of Drug Delivery to the Brain. *Pharm.Res.* **2008,** 25, 1737-1750.
34. Hammarlund-Udenaes M, Bredberg U and Friden M. Methodologies to assess brain drug delivery in lead optimization. *Curr Top Med Chem.* **2009,** 9, 148-162.
35. Patlak CS, Blasberg RG and Fenstermacher JD. Graphical evaluation of blood-to-brain transfer constants from multiple-time uptake data. *Journal of Cerebral Blood Flow & Metabolism.* **1983,** 3, 1-7.
36. Takasato Y, Rapoport SI and Smith QR. An in situ brain perfusion technique to study cerebrovascular transport in the rat. *Am.J.Physiol.* **1984,** 247, H484-93.
37. Oldendorf WH. Measurement of brain uptake of radiolabeled substances using a tritiated water internal standard. *Brain Res.* **1970,** 24, 372-376.
38. Syvanen S, Xie R, Sahin S and Hammarlund-Udenaes M. Pharmacokinetic consequences of active drug efflux at the blood-brain barrier. *Pharm.Res.* **2006,** 23, 705-717.

39. Kakee A, Terasaki T and Sugiyama Y. Brain efflux index as a novel method of analyzing efflux transport at the blood-brain barrier. *Journal of Pharmacology & Experimental Therapeutics.* **1996,** 277, 1550-1559.
40. Elmquist WF and Sawchuk RJ. Application of microdialysis in pharmacokinetic studies. *Pharm.Res.* **1997,** 14, 267-288.
41. de Lange EC, de Boer BA and Breimer DD. Microdialysis for pharmacokinetic analysis of drug transport to the brain. *Adv.Drug Deliv.Rev.* **1999,** 36, 211-227.
42. Hammarlund-Udenaes M. The use of microdialysis in CNS drug delivery studies. Pharmacokinetic perspectives and results with analgesics and antiepileptics. *Adv.Drug Deliv.Rev.* **2000,** 45, 283-294.
43. Bungay PM, Morrison PF and Dedrick RL. Steady-state theory for quantitative microdialysis of solutes and water in vivo and in vitro. *Life Sciences.* **1990,** 46, 105-119.
44. Groothuis DR, Ward S, Schlageter KE, Itskovich AC, Schwerin SC, Allen CV*, et al*. Changes in blood-brain barrier permeability associated with insertion of brain cannulas and microdialysis probes. *Brain Res.* **1998,** 803, 218-230.
45. de Lange EC, Danhof M, de Boer AG and Breimer DD. Critical factors of intracerebral microdialysis as a technique to determine the pharmacokinetics of drugs in rat brain. *Brain Research.* **1994,** 666, 1-8.
46. Kalvass JC and Maurer TS. Influence of nonspecific brain and plasma binding on CNS exposure: implications for rational drug discovery. *Biopharm.Drug Dispos.* **2002,** 23, 327-338.
47. Mano Y, Higuchi S and Kamimura H. Investigation of the high partition of YM992, a novel antidepressant, in rat brain - in vitro and in vivo evidence for the high binding in brain and the high permeability at the BBB. *Biopharmaceutics & Drug Disposition.* **2002,** 23, 351-360.
48. Khor SP, Bozigian H and Mayersohn M. Potential error in the measurement of tissue to blood distribution coefficients in physiological pharmacokinetic modeling. Residual tissue blood. II. Distribution of phencyclidine in the rat. *Drug Metabolism & Disposition.* **1991,** 19, 486-490.
49. Preston E and Haas N. Defining the lower limits of blood-brain barrier permeability: factors affecting the magnitude and interpretation of permeability-area products. *J.Neurosci.Res.* **1986,** 16, 709-719.
50. Smith QR, Ziylan YZ, Robinson PJ and Rapoport SI. Kinetics and distribution volumes for tracers of different sizes in the brain plasma space. *Brain Res.* **1988,** 462, 1-9.
51. Reichel A, Begley DJ and Abbott NJ. An overview of in vitro techniques for blood-brain barrier studies. *Methods Mol.Med.* **2003,** 89, 307-324.
52. Nicolazzo JA, Charman SA and Charman WN. Methods to assess drug permeability across the blood-brain barrier. *J.Pharm.Pharmacol.* **2006,** 58, 281-293.

53. Avdeef A. The rise of PAMPA. *Expert Opin.Drug Metab.Toxicol.* **2005,** 1, 325-342.
54. Matsson P. ATP-Binding cassette efflux transporters and passive membrane permeability in drug absorption and disposition. *Digital Comprehensive Summaries of Uppsala Dissertations from the Faculty of Pharmacy.* **2007,** 67, 68 pp.
55. Wold S. PLS-regression: a basic tool of chemometrics. *Chemometr Intell Lab.* **2001,** 58, 109-130.
56. Wold S. Validation of QSAR´s. *Quant. Struct.- Act. Relat.* **1991,** 10, 191-193.
57. Young RC, Mitchell RC, Brown TH, Ganellin CR, Griffiths R, Jones M*, et al*. Development of a new physicochemical model for brain penetration and its application to the design of centrally acting H2 receptor histamine antagonists. *J.Med.Chem.* **1988,** 31, 656-671.
58. Abraham MH, Chadha HS and Mitchell RC. Hydrogen bonding. 33. Factors that influence the distribution of solutes between blood and brain. *J.Pharm.Sci.* **1994,** 83, 1257-1268.
59. Abraham MH, Ibrahim A, Zissimos AM, Zhao YH, Comer J and Reynolds DP. Application of hydrogen bonding calculations in property based drug design. *Drug Discov.Today.* **2002,** 7, 1056-1063.
60. Abraham MH. The factors that influence permeation across the blood-brain barrier. *Eur.J.Med.Chem.* **2004,** 39, 235-240.
61. Luco JM. Prediction of the brain-blood distribution of a large set of drugs from structurally derived descriptors using partial least-squares (PLS) modeling. *J.Chem.Inf.Comput.Sci.* **1999,** 39, 396-404.
62. Osterberg T and Norinder U. Prediction of polar surface area and drug transport processes using simple parameters and PLS statistics. *J.Chem.Inf.Comput.Sci.* **2000,** 40, 1408-1411.
63. Bendels S, Kansy M, Wagner B and Huwyler J. In silico prediction of brain and CSF permeation of small molecules using PLS regression models. *Eur.J.Med.Chem.* **2008,** 43, 1581-1592.
64. Clark DE. In silico prediction of blood-brain barrier permeation.[see comment]. *Drug Discov.Today.* **2003,** 8, 927-933.
65. Palm K, Stenberg P, Luthman K and Artursson P. Polar molecular surface properties predict the intestinal absorption of drugs in humans. *Pharm.Res.* **1997,** 14, 568-571.
66. Kelder J, Grootenhuis PD, Bayada DM, Delbressine LP and Ploemen JP. Polar molecular surface as a dominating determinant for oral absorption and brain penetration of drugs. *Pharm.Res.* **1999,** 16, 1514-1519.
67. de Lange EC and Danhof M. Considerations in the use of cerebrospinal fluid pharmacokinetics to predict brain target concentrations in the clinical setting: implications of the barriers between blood and brain. *Clin.Pharmacokinet.* **2002,** 41, 691-703.

68. Lee CM and Farde L. Using positron emission tomography to facilitate CNS drug development. *Trends Pharmacol.Sci.* **2006,** 27, 310-316.
69. Skold C, Winiwarter S, Wernevik J, Bergstrom F, Engstrom L, Allen R*, et al*. Presentation of a structurally diverse and commercially available drug data set for correlation and benchmarking studies. *J.Med.Chem.* **2006,** 49, 6660-6671.
70. Umetrics AB, Box 7960, SE-90717 Umeå, Sweden. SIMCA P+, 11.5 **2006.**
71. Wan H and Rehngren M. High-throughput screening of protein binding by equilibrium dialysis combined with liquid chromatography and mass spectrometry. *Journal of Chromatography.A.* **2006,** 1102, 125-134.
72. Habgood MD, Sedgwick JE, Dziegielewska KM and Saunders NR. A developmentally regulated blood-cerebrospinal fluid transfer mechanism for albumin in immature rats. *J.Physiol.* **1992,** 456, 181-192.
73. Wan H, Holmen AG, Wang Y, Lindberg W, Englund M, Nagard MB*, et al*. High-throughput screening of pKa values of pharmaceuticals by pressure-assisted capillary electrophoresis and mass spectrometry. *Rapid Commun.Mass Spectrom.* **2003,** 17, 2639-2648.
74. Altman DG and Bland JM. Measurement in medicine: the analysis of method comparison studies. *The statistician.* **1983,** 32, 307-317.
75. Bland JM and Altman DG. Measuring agreement in method comparison studies. *Stat.Methods Med.Res.* **1999,** 8, 135-160.
76. SAS Institute Inc., Cary, NC, USA. SAS/STAT. The SAS Package.
77. Wikipedia. Propagation of uncertainty, 2010. http://en.wikipedia.org/wiki/Propagation_of_uncertainty.
78. Shore PA, Brodie BB and Hogben CA. The gastric secretion of drugs: a pH partition hypothesis. *J.Pharmacol.Exp.Ther.* **1957,** 119, 361-369.
79. Liu X, Van Natta K, Yeo H, Vilenski O, Weller PE, Worboys PD*, et al*. Unbound drug concentration in brain homogenate and cerebral spinal fluid at steady state as a surrogate for unbound concentration in brain interstitial fluid. *Drug Metab.Dispos.* **2009,** 37, 787-793.
80. Schinkel AH, Wagenaar E, Mol CA and van Deemter L. P-glycoprotein in the blood-brain barrier of mice influences the brain penetration and pharmacological activity of many drugs. *J.Clin.Invest.* **1996,** 97, 2517-2524.
81. Seelig A and Landwojtowicz E. Structure-activity relationship of P-glycoprotein substrates and modifiers. *Eur.J.Pharm.Sci.* **2000,** 12, 31-40.
82. Rao VV, Dahlheimer JL, Bardgett ME, Snyder AZ, Finch RA, Sartorelli AC*, et al*. Choroid plexus epithelial expression of MDR1 P glycoprotein and multidrug resistance-associated protein contribute to the blood-cerebrospinal-fluid drug-permeability barrier. *Proc.Natl.Acad.Sci.U.S.A.* **1999,** 96, 3900-3905.
83. Begley DJ. ABC transporters and the blood-brain barrier. *Curr.Pharm.Des.* **2004,** 10, 1295-1312.

84. Okura T, Hattori A, Takano Y, Sato T, Hammarlund-Udenaes M, Terasaki T*, et al*. Involvement of the pyrilamine transporter, a putative organic cation transporter, in blood-brain barrier transport of oxycodone. *Drug Metab.Dispos.* **2008,** 36, 2005-2013.
85. Andre P, Debray M, Scherrmann JM and Cisternino S. Clonidine transport at the mouse blood-brain barrier by a new H+ antiporter that interacts with addictive drugs. *J.Cereb.Blood Flow Metab.* **2009,** 29, 1293-1304.
86. Neuwelt E, Abbott NJ, Abrey L, Banks WA, Blakley B, Davis T*, et al*. Strategies to advance translational research into brain barriers. *Lancet Neurol.* **2008,** 7, 84-96.
87. Chiro GD, Hammock MK and Bleyer WA. Spinal descent of cerebrospinal fluid in man. *Neurology.* **1976,** 26, 1-8.

Acta Universitatis Upsaliensis

Digital Comprehensive Summaries of Uppsala Dissertations from the Faculty of Pharmacy 128

Editor: The Dean of the Faculty of Pharmacy

A doctoral dissertation from the Faculty of Pharmacy, Uppsala University, is usually a summary of a number of papers. A few copies of the complete dissertation are kept at major Swedish research libraries, while the summary alone is distributed internationally through the series Digital Comprehensive Summaries of Uppsala Dissertations from the Faculty of Pharmacy. (Prior to January, 2005, the series was published under the title "Comprehensive Summaries of Uppsala Dissertations from the Faculty of Pharmacy".)

Distribution: publications.uu.se
urn:nbn:se:uu:diva-130230

ACTA
UNIVERSITATIS
UPSALIENSIS
UPPSALA
2010